ISTANBUL TECHNICAL UNIVERSITY ★ GRADUATE SCHOOL OF SCIENCE ENGINEERING AND TECHNOLOGY

RECONSTRUCTION OF OBJECTS LOCATED IN THREE PART PLANARLY LAYERED MEDIA

M.Sc. THESIS

Fatih ERDEM

Department of Electronics and Telecommunication Engineering

Telecommunication Engineering Programme

JUNE 2012

ISTANBUL TECHNICAL UNIVERSITY ★ GRADUATE SCHOOL OF SCIENCE ENGINEERING AND TECHNOLOGY

RECONSTRUCTION OF OBJECTS LOCATED IN THREE PART PLANARLY LAYERED MEDIA

M.Sc. THESIS

Fatih ERDEM
(504091363)

Department of Electronics and Telecommunication Engineering

Telecommunication Engineering Programme

Thesis Advisor: Prof. Dr. İbrahim AKDUMAN

JUNE 2012

İSTANBUL TEKNİK ÜNİVERSİTESİ ★ FEN BİLİMLERİ ENSTİTÜSÜ

ÜÇ TABAKALI ORTAM İÇERİSİNE GÖMÜLÜ CİSİMLERİN GÖRÜNTÜLENMESİ

YÜKSEK LİSANS TEZİ

Fatih ERDEM
(504091363)

Elektronik ve Haberleşme Münedisliği Anabilim Dalı

Haberleşme Mühendisliği Programı

Tez Danışmanı: Prof. Dr. İbrahim AKDUMAN

HAZİRAN 2012

Fatih Erdem, a **M.Sc.** student of ITU **Institute of Science and Technology** student ID 504091363, successfully defended the **thesis** entitled “**RECONSTRUCTION OF OBJECTS LOCATED IN THREE PART PLANARLY LAYERED MEDIA**”, which he prepared after fulfilling the requirements specified in the associated legislations, before the jury whose signatures are below.

Thesis Advisor :	**Prof. Dr. İbrahim AKDUMAN** İstanbul Technical University	....
Jury Members :	**Prof. Dr. Ali YAPAR** İstanbul Technical University	....
	Asst. Prof. Dr. Lale Tükenmez ERGENE İstanbul Technical University	....

Date of Submission : 3 May 2012
Date of Defense : 8 June 2012

FOREWORD

I would like to thank Prof. Dr. İbrahim Akduman for his supervision and support during my master study. I would also like to thank members of İTÜ Electormagnetics Research Group for their support. I would especially thank to the members Mehmet Abbak, Birol Arslanyürek, Dr. Mehmet Çayören and Tolga Ulaş Gürbüz for making valuable discussions with me.
I would like to express my appreciation to TÜBİTAK-BİDEB that motivates and financially aids me during my master study.

April 2012

Fatih Erdem
(Electronics Engineer)

TABLE OF CONTENTS

Page

ABBREVIATIONS

CSI : Contrast Source Inversion
MOM : Method of Moments
FEM : Finite Element Method
FIP : Fourier Inversion Path

LIST OF FIGURES

Page

RECONSTRUCTION OF OBJECTS LOCATED IN THREE PART PLANARLY LAYERED MEDIA

SUMMARY

In this study, the problem of reconstructing the location and the shape of a buried object in a three part planarly layered media is considered. The problem is studied in two dimensions serving as a prestudy for three-dimensional problems requiring more advanced math and high computational capability. Contrast Source Inversion method (CSI) which is one of the most effective inversion algorithms is employed to solve the inverse problems. To this aim, the CSI method is applied for the objects located in infinite medium first in order to verify correct implementation of the method. Then, the method is applied for objects located in a three part planarly layered media. In infinite medium case, the forward problem is solved using Method of Moment (MOM) to produce synthetic data and the results validated by analytical solution and Finite Element Method (FEM) solution. For the inverse problem, the reconstruction domain is illuminated by planewaves impinging on to the domain circumferentially. Receive points are located being equally arranged in a full circle. Satisfactory results are obtained in the infinite medium case. In stratified media case, the forward problem is solved using MOM by utilizing the Green's functions pertaining to three part planarly layered media. It is checked that one component of the Green's functions used in the forward solution is calculated correctly through the Fourier inversion path by comparing the results with available analytical expressions. This check also provided a powerful evidence indicating that the other components having similar analytical behavior are calculated correctly through the same integral path. The reconstruction domain is illuminated by down going planewaves and receive points are located in the upper half space which is the only accessible media. The effect of linearly and circularly arranged receive points on the reconstruction performance is tested. The method is studied for different cases. The reconstruction performance for small and close objects are investigated. The performance is degraded comparing to infinite medium case but obtained results showed that Contrast Source Inversion method can be applied to reconstruct objects located in a three part planarly layered media.

ÜÇ TABAKALI ORTAM İÇERİSİNE GÖMÜLÜ CİSİMLERİN GÖRÜNTÜLENMESİ

ÖZET

Yanına yaklaşılamayan cisimlerin elektromagnetik dalgalarla görüntülenmesi elektromagnetik alanının en gelişmiş uygulamalarından birisidir. Günümüzde kullanılagelen görüntüleme sistemlerine bakıldığında askeri ve sivil alanda radar temelli sistemler, medikal uygulamalarda röntgen ışını temelli sistemler görülmektedir. Bu sistemlerde yüksek enerji kullanılmasına rağmen ancak düşük çözünürlüklü görüntüler elde edilebilmektedir. Özellikle medikal uygulamalarda hastaları yüksek enerjiye maruz bırakmadan daha yüksek çözünürlüklü görüntüler elde edebilen görüntüleme sistemlerine olan ihtiyaç günümüzde iyice belirgin hale gelmiştir. Göğüs kanseri gibi erken teşhisin kritik olduğu vakalarda daha iyi çözünürlüklü görüntüleme yapılması hastaların hayatını kurtarabilmektedir. Mikrodalga görüntüleme olarak adlandırılan görüntüleme sistemi, çok düşük güçlü elektromagnetik dalgalar ile yüksek çözünürlüklü görüntüler elde etmeyi amaçlayan bir görüntüleme sistemdir.

Literatürde görüntüleme işlemi elektromagnetik ters probleme karşı düşmektedir. Elektromagnetikte problemler, düz saçılma problemleri ve ters saçılma problemleri olarak iki kategoriye ayrılabilir. Bilinen bir cismin bilinen bir kaynak ile aydınlatılması sonucu oluşacak saçılan alanın belirlenmesi problemi düz problem olarak tanımlanır. Bilinmeyen bir cismin bilinen bir kaynak ile aydınlatılması ve oluşan saçılan alan bilgisi kullanılarak bilinmeyen cismin geometrik ve fiziksel özelliklerinin belirlenmesi problemi ise ters saçılma problemi olarak tanımlanır. Ters saçılma problemleri düz saçılma problemlerine göre çok daha karmaşık ve gelişmiş yöntemler gerektirir. Bir ters saçılma probleminde çözümün varlığı, tekliği konuları dahi araştırma konusu teşkil etmektedir. Son yarım asırda ters saçılma problemlerine yönelik çeşitli algoritmalar geliştirilmiştir. Bu algoritmalar doğrusal ve doğrusal olmayan algoritmalar olarak basitçe sınıflandırılabilir. Doğrusal olmayan algoritmalar problemin doğasına daha uygun olduklarından daha verimli sonuçlar üretebilmektedir. Doğrusal olmayan algoritmalar da kendi içerisinde lokal ve global algoritmalar olarak sınıflandırılabilir. Lokal algoritmalar belirlenen bir fonksiyoneli belirli bir bölgede minimize etmeyi amaçlar, bu algoritmalarda başlangıç tahminleri sonucun yakınsaması için kritik öneme sahiptir. Global algoritmalar ise belirlenen fonksiyonelin global minimum değerini bulmayı hedefler. Bu çalışmada, ters problemlerin çözümünde kullanılacak olan "Contrast Source Inversion" metodu doğrusal olmayan lokal bir algoritma olup bu kategoride öne çıkan yöntemlerden birisidir.

İkinci bölümde düz problemlerin Green fonksiyonları yardımıyla Moment Metodu ile çözümü ele alınmıştır. Düz problem çözümünde Moment Metodu kullanıldığında farklı geometriler için sadece Green fonksiyonlarının değiştiği, çözüm yönteminde bir değişiklik olmadığı vurgulanmıştır. Saçılan alan için yazılan Helmholtz denklemi, Green fonksiyonları yardımıyla integral denklemi olarak ifade edilmiş ve düz problem ikinci türden Fredholm integral denklemine dönüştürülmüştür. Bu denklem de uygun hücre boyutları üzerinden ayrıklaştırılmış ve düz problem çözümü elde edilmiştir. Örnek bazı durumlar için farklı yöntemlerle çözülen düz problem sonuçları üçüncü bölümde verilmiştir.

Dördüncü bölümde ise ters problem ve "Contrast Source Inversion" metodu ele alınmıştır. Bir optimizasyon algoritması olarak düşünülebilen yöntemin uygulama adımları gösterilmiştir.

Çalışmanın nihai amacı üç parçalı bir ortam içerisine gömülü cisimlerin elektromagnetik dalgalar ile görüntülenmesidir. Bu amaca yönelik "Contrast Source Inversion" metodu öncelikle sonsuz uzay içerisine yerleştirilmiş cisimlerin görüntülenmesi için uygulanmıştır ve başarılı sonuçlar elde edilmiştir. Ters problem çalışması için gereken saçılan alan verileri düz problemin Moment Metodu ile çözülmesiyle elde edilmiştir. Sonsuz uzay durumunda elde edilen saçılan alan verisinin doğruluğu, analitik çözümlerle ve sonlu eleman analizi çözümü ile karşılaştırma yapılarak kontrol edilmiştir. Elde edilen saçılan alan verileriyle yapılan ters çözümlerde iyi sonuçlar alınmış ve sonsuz uzay durumunda yöntemin doğru uygulandığı görülmüştür.

Çalışmaya konu olan üç parçalı uzay, düzlemsel sınırlarla ayrılmış homojen, kayıpsız ortamlardan oluşmaktadır. Parçalı uzay durumu için Green fonksiyonları Fourier dönüşümü kullanılarak elde edilmiştir. Yatay eksende alınan Fourier dönüşümü ile Green fonksiyonları için yazılan Helmholtz denklemi bağımsız değişkeni parçalı eksen olan adi diferansiyel denkleme dönüştürülmüş ve spektral Green fonksiyonları elde edilmiştir. Spektral Green fonksiyonları içerdikleri kompleks fonksiyonların tanımları dikkate alınarak belirlenen Fourier ters dönüşüm integral yolu üzerinden integre edilerek uzaysal Green fonksiyonları elde edilmiştir. Spektral Green fonksiyonlarının integral yolu üzerindeki davranışı incelenmiş, sayısal integrallerde integral değişkeninin sıklığı değiştirilerek integral sonucunun yakınsaklığı ve sonuçların fiziksel durumla örtüştüğü kontrol edilmiştir.

Parçalı uzay için düz problem sonuçlarının doğruluğu, Fourier ters dönüşüm integral yolu üzerinden hesaplanan Green fonksiyonunun bir bileşeninin analitik ifadeyle karşılaştırılmasıyla kontrol edilmiştir. Bahsi geçen bileşen Hankel fonksiyonun spektral gösterimidir. Böylece, analitik davranış olarak büyük farklılık göstermeyen Green fonksiyonu diğer bileşenlerinin de sayısal integralinin doğru hesaplandığı düşünülmüştür. Boş uzay durumuna göre aydınlatmanın sadece üst uzaydan yapılması ve saçılan alanın sadece üst uzayda ölçülebiliyor olması görüntüleme performansını olumsuz yönde etkilemektedir. Elde edilen saçılan alan verileriyle yapılan ters çözümlerde boş uzay durumundaki kadar olmasa da iyi sonuçlar elde edilmiştir. Genel olarak, parçalı uzayda elde edilen görüntülerin aydınlatmanın sadece üstten yapılabilmesi sebebiyle gölgeli oluştuğu gözlenmiştir. Cisim boyutları ve birden fazla cisim durumunda cisimlerin birbirine yakınlığının görüntüleme performansına etkisi gözlenmiştir. Görüntüleme bölgesinin büyüklüğünün görüntüleme çözünürlüğüne etkisi gözlenmiştir. Görüntüleme bölgesi boyutlarına yaklaşmayacak kadar küçük ve dalgaboyunun onda birinden daha büyük boyutta cisimlerin daha iyi görüntülendiği gözlenmiştir. Dalgaboyunun onda birinden daha küçük cisimlerin elektriksel özelliklerinin doğru tespit edilemediği ancak yerlerinin

tespit edildiği ve bazı durumlarda cisim görüntüsünün aynalı olarak elde edildiği gözlenmiştir.
İki cisim durumunda cisimlerin görüntüleme bölgesinin zıt köşelerine yakın olduğu hallerde ayırt edilebildiği, birbirlerine yakınlaştığı hallerde ise tek cisim gibi görüntülendiği gözlenmiştir. İki cisim durumunda en kötü görüntüleme performansının cisimler dikey olarak hizalandığında oluştuğu gözlenmiştir. Cisim permitivitesinin ortama çok yakın veya çok uzak olmasının görüntüleme performansını olumsuz yönde etkilediği gözlenmiştir. Kontrast değeri bire yaklaştıkça veya üç-dört değerini aştıkça cisim görüntüsünün esas yerinden sapma yaptığı ve bazı durumlarda aynalanmış olarak görüntülendiği gözlenmiştir.
Ters problem algoritmalarının objektif bir biçimde değerlendirilmesi düz problem çözümünde kullanılan yöntemlerin ters algoritmalarda yer almamasını gerektirmektedir. Aksi durumda, düz problem çözümünde yapılan hataların ters problem çözümünde ortaya çıkmama veya sürpriz iyi sonuçlar elde etme riski vardır. Bu risk literatürde "inverse crime" olarak adlandırılmaktadır. Bu durumdan kaçınmak için düz problem çözümünün tamamen farklı bir yöntemle yapılması gerekmektedir. Bu çalışmada sonsuz uzay durumu için düz problem analitik yöntemlerle ve sonlu eleman analizi ile çözülebilmiştir ancak üç parçalı uzay durumu için düz problem sadece Moment Metodu ile çözülmüştür. Parçalı uzay durumunda sonlu eleman analiz çözümlerinin sınır koşullarının tam doğru yazılamaması sebebiyle düzlem dalgaların gelme açısı arttıkça kararsız çözümler elde edilmiştir dolayısıyla sonlu elemanlar yöntemi kullanılamamıştır. Moment Metodu çalışmaya konu olan ters algoritma içerisinde de kullanıldığından algoritma performansının objektif değerlendirilememesi riski bulunmaktadır. Parçalı uzay durumu için düz problemin doğru kurulduğu ve çözüldüğüne dair kanıtlar ortaya konmuş olsa da bahsi geçen risk bulunmaktadır. Bu riske rağmen elde edilen sonuçlar mantıklı olup "Contrast Source Inversion" metodunun üç parçalı uzay için uygulanabilir olduğu görülmüştür.

1. INTRODUCTION

Imaging of inaccessible objects is one of the most sophisticated applications of the electromagnetics. Radar based systems and Xrays imaging systems those are rontgen, mammography and conventional tomography in medical imaging are most popular imaging systems.

The common drawbacks of these systems are excessive power use and inadequate image resolution. Radar systems can only form low-resolution images despite their high power use. In medical imaging; although X-rays' harmful effects on human cells could not be explored clearly yet, nobody wants to be exposed such a high power. Furthermore, X-ray imaging especially in mammography may not give detailed enough information in some cases and this risks patients those can be treated well if early diagnosis is achieved.

High power exposure and low resolution of today's imaging systems encourages researchers to work on microwave imaging (MWI). MWI offers high resolution imaging with low power electormagnetic waves. In addition to aforementioned applications, MWI can be extended to many medical, industrial and military applications.

In electromagnetics literature, the term imaging corresponds to inverse scattering problem. Problems in electromagnetics can be categorized as forward scattering and inverse scattering problems those are called forward and inverse problems shortly. A known object(s) located in a known environment is illuminated by a known electromagnetic source, how the target object(s) scatters is defined as forward scattering problem. An unknown object(s) located in a known inaccessible background media is illuminated by a known electromagnetic source, determination of geometrical and physical properties of the unknown object(s) from scattered data collected at accessible points is defined as inverse scattering problem. Human vision is an everyday example of inverse scattering problem, the brain reconstruct three-dimensional objects from the knowledge of scattered light impinging on the retinas.

Investigation of the inverse problems forces researchers to work on forward problems first. Results of accurately solved forward problems make researchers to work with reliable data so that inversion algorithms can be studied well.

As it may be guessed, inverse problems are much more sophisticated than forward problems. In forward problems, as they are well posed, analytical and numerical methods such as Method of Moments (MOM), Finite Element Method (FEM), Finite Difference Time Domain (FDTD) method can be employed. On the other hand, due to their ill-posed nature, inverse problems require advanced algorithms.

Inversion algorithms can be classified as linear and nonlinear algorithms. Linear algorithms simplify the inverse problem by making some approximations. They are most early developed algorithms and have limited application areas due to their restrictions. Linear diffraction tomography algorithm and Born approximation are popular linear methods. On the other hand, nonlinear methods keep nonlinear nature of the inverse problem and bring more accurate results. They are mathematically more complex and carried out via iterations. Nonlinear methods cast the inverse problem as an optimization problem and they can also be classified as local and global inversion algorithms. Newton–Kantorovich algorithm [1], the conjugate-gradient method, the modified gradient method [2] and the Contrast Source Inversion (CSI) [3] method are outstanding local inversion algorithms those seek local minimum of a predefined cost functional. Genetic algorithms and neural networks are popular examples of global inversion algorithms.

Aforementioned nonlinear local inversion algorithms have been developed for past three decades and Contrast Source Inversion (CSI) method is the most outstanding method among them [4].

Electromagnetic problems in the real life are three-dimensional problems. Three-dimensional problems require advanced mathematics and high computational capability. It is necessary to study on lower-dimensional problems before studying three-dimensional problems. Once the concepts in two-dimensional cases are established well, the studies can be extended to three-dimensional problems. Moreover, there may be some cases in real life those cause acceptable errors when modeled in two dimension. Wide walls, long pipes, large areas can be thought as two-dimensional objects in the modeling.

The wave motion is governed by the wave equation that is a vector partial differential equation defined in the time domain in three dimensions. In time harmonic case, the wave equation reduces to Helmholtz equation that is also a vector partial differential equation. It also reduces to scalar partial differential equation if the field variable is directed in one direction only.

$$\Delta E(x,y) + k^2(x,y) \cdot E(x,y) = 0 \qquad \textbf{(1.1)}$$

Equation 1.1 is scalar Helmholtz equation written for TMz electric fields where k is propagation constant of the medium. This equation is the main equation to solve forward problems in the thesis. Analytical methods such as separation of variables can be employed to solve the Helmholtz equation for some canonical cases. However, when arbitrarily shaped scattering objects take into play, numerical methods such as MOM, FEM, FDTD should be employed. In this work, MOM is used as primary numerical method for forward problems. In addition to MOM, FEM is employed as a collaborating numerical method to validate MOM results. FEM solutions are obtained using a simple FEM tool, FreeFEM [5].

In order to apply MOM, Helmholtz equation is converted to integral equation that is a Fredholm integral equation of the second kind by utilizing the Green's functions. Then, the integral equation is discretized.

In inverse problems, Contrast Source Inversion method is used. The method is applied for the objects located in infinite medium first as depicted in the paper from which the method originates. Then, it is applied for the objects located in three part planarly layered media.

The thesis is organized as follows, Section 2 depicts forward problems and Section 3 gives related numerical results. In Section 4, inverse problems are studied and numerical results are given in Section 5.

$e^{-i \cdot \omega \cdot t}$ is understood time factor for phasor calculations.

1.1 Purpose of the Work

The aim of this work is to study on application of Contrast Source Inversion method to reconstruct objects located in a three part planarly layered media.

2. FORWARD PROBLEMS FOR OBJECTS LOCATED IN THREE PART PLANARLY LAYERED MEDIA

This section depicts solution of two-dimensional forward scattering problems. The scattered filed data is necessary for the inverse problem study. The data will be obtained synthetically by solving the forward problem. As it is mentioned in Section 1, MOM will be used as primary numerical method to solve the forward problems. The cases for objects located in infinite medium and objects located in three part planarly layered media will be both studied. In MOM, different mediums differ Green's functions only in the solution procedure. Once Green's functions pertaining to the medium are obtained, the rest of the problem is straightforward. Therefore, a simple geometry will be used to illustrate the forward solution procedure.

2.1 Formulation of the Forward Scattering Problem

An infinite dielectric cylinder is located along the z-axis in a linear, isotropic and lossless media as shown in Figure 2.1. The permittivity of the object and the background medium are not necessarily homogeneous. The object is illuminated by a TMz planewave propagating in an arbitrary direction.

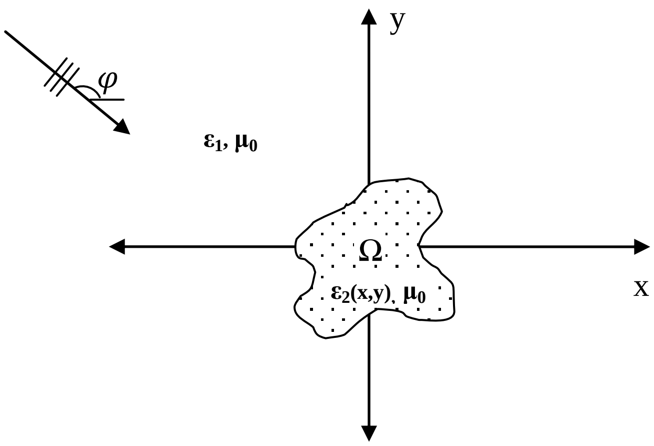

Figure 2.1 : An example geometry for the forward problem.

The Helmholtz equation reduces to scalar one because the electric field has z component only. The total electric field satisfies the Helmholtz equation shown in (2.1)

$$\Delta E(x,y) + k^2(x,y) \cdot E(x,y) = 0 \tag{2.1}$$

where k is propagation constant being defined by $k^2 = \omega^2 \varepsilon\mu + i\omega\sigma\mu$

$$k(x,y) = \begin{cases} k_1, & (x,y) \notin \Omega \\ k_2, & (x,y) \in \Omega \end{cases} \tag{2.2}$$

and the incident field satisfies (2.3).

$$\Delta E^i + k_1^2 \cdot E^i = 0 \tag{2.3}$$

The coordinate indices (x,y) and vector cap placed above a vector will be dropped to simplify equations i.e. $E = E(x,y) \cdot \vec{a}_z$ throughout the thesis. They will be emphasized when necessary.

It can also be stated that the total field at any point equal to summation of the incident and the scattered field at that point as shown in (2.4).

$$E^i + E^s = E \tag{2.4}$$

Two terms can be added and subtracted in (2.1), it becomes (2.5).

$$\Delta E + k^2 \cdot E + k_1^2 \cdot E^i - k_1^2 \cdot E^i + k_1^2 \cdot E^s - k_1^2 \cdot E^s = 0 \tag{2.5}$$

using (2.4)

$$\Delta\left(E^i + E^s\right) + k_1^2 \cdot E^i - k_1^2 \cdot E^i + k_1^2 \cdot E^s - k_1^2 \cdot E^s = -k^2 \cdot E \tag{2.6}$$

$$\Delta E^s - k_1^2 \cdot E + k_1^2 \cdot E^s = -k^2 \cdot E \tag{2.7}$$

$$\Delta E^s + k_1^2 \cdot E^s = -(k^2 - k_1^2) \cdot E \tag{2.8}$$

and using the definition of the object function given in (2.9), (2.8) can be expressed as (2.10).

$$\chi(x,y) = \frac{k^2(x,y) - k_1^2}{k_1^2} = \varepsilon_r(x,y) - 1 \qquad \textbf{(2.9)}$$

The object function is also called as contrast as it will be referred in Section 3.

$$\Delta E^s + k_1^2 \cdot E^s = -k_1^2 \cdot \chi \cdot E \qquad \textbf{(2.10)}$$

It is seen that the polarization current induced in the cylinder can be thought as source current of the scattered field, this approach is called volumetric equivalence principle [6].

It is also known that, by definition, the solution of (2.11) in a medium gives Green's function of the medium.

$$\Delta G(x,y;x',y') + k_1^2 \cdot G(x,y;x',y') = -\delta(x) \cdot \delta(y) \qquad \textbf{(2.11)}$$

Green's functions enable us to write the solution of (2.8) in the integral form as in (2.12).

$$E^s(x,y) = \int_{\Omega} k_1^2(x',y') \cdot \chi(x',y') \cdot E\,(x',y') \cdot G(x,y;x',y') \cdot dx' \cdot dy' \qquad \textbf{(2.12)}$$

where (x,y) and (x',y') are the coordinates of the observation and source point, respectively. The apostrophes are used to indicate source locations throughout the thesis.

Integration surface Ω indicates surface area on the cross section of the cylinder. The term $k_1^2(x',y')$ can be taken out of the integral if it does not vary along the region Ω, it will be assumed that it does not vary along the region Ω from now on.

In this manner, one can write scattered field anywhere, either in the object or outside of it, in terms of the electric field in the object.

If (2.12) is substituted in (2.4), one can end up with domain integral equation (2.13) which is a Fredholm integral equation of the second kind.

$$E(x,y) = E^i(x,y) + k_1^2 \int_{\Omega} \chi(x',y') \cdot E\,(x',y') \cdot G(x,y;x',y') \cdot dx' \cdot dy' \qquad \textbf{(2.13)}$$

The next step is discretization of the domain integral equation. The domain Ω will be subdivided into such small square cells that the dielectric constant and the field variation over a cell can be neglected. The cells do not have to be same sized, they can be fined regionally. Edge dimensions should not exceed $0.2 \cdot \lambda/\sqrt{\varepsilon_r}$ for accurate results [7].

(2.13) is forced to be hold at the center of each cell m and the following equation is obtained.

$$E_m = E_m^i + k_1^2 \cdot \sum_{n=1}^{N} \chi_n \cdot E_n \int_{cell\,n} G(x, y; x', y') \cdot dx' \cdot dy' \qquad \textbf{(2.14)}$$

where N represents number of cells and E represents the electric field at the center of a cell. One can write (2.14) for each cell and end up with N unknowns, the field variables E, and N equations. The system of linear equations can be expressed in a matrix equation (2.15)

$$(I - D) \cdot E = E^i \qquad \textbf{(2.15)}$$

where I represents NxN identity matrix and D can be expressed as (2.16).

$$D_{mn} = k_1^2 \cdot \chi_n \cdot \int_{cell\,n} G(x, y; x', y') \cdot dx' \cdot dy' \qquad \textbf{(2.16)}$$

(2.15) can be stated in a more compact form as in (2.17).

$$C \cdot E = E^i \qquad \textbf{(2.17)}$$

The unknown electric field variables can be found by inverting the matrix C.

$$E = C^{-1} \cdot E^i \qquad \textbf{(2.18)}$$

Once the electric field over the object is found, scattered field at any point can be calculated using (2.19).

$$E^s(x, y) = k_1^2 \cdot \sum_{n=1}^{N} \chi_n \cdot E_n \int_{cell\,n} G(x, y; x', y') \cdot dx' \cdot dy' \qquad \textbf{(2.19)}$$

A complete solution procedure for the forward problem has been illustrated but no Green's functions have been mentioned yet. It can be deduced that forward scattering problems for objects located in different media necessitates different Green's functions only and do not change the solution procedure.

In the example case, the background medium is infinite and its Green's function is solution of (2.11) with the condition k_1^2 is the same everywhere. The Green's function is given by (2.20).

$$G(x, y; x', y') = \frac{i}{4} \cdot H_0^{(1)}\left(k_1 \cdot \sqrt{(x - x')^2 + (y - y')^2}\right) \qquad \textbf{(2.20)}$$

where (x,y) and (x',y') are the coordinates of the observation and source point, respectively.

It should be noted that surface integration of the Green's function given in (2.20) over a computation cell is problematic. A closed form solution of the integration of the Hankel function over a square or rectangular cell is not known. Furthermore, we encounter a singular point in the integration region when the source and the observation cells are the same. Analytical expressions figuring out the both problems can be found in [7].

2.2 The Problem Geometry and Green's Functions for the Forward Problem

The geometry of the forward problem is three part planarly layered media and the object is located in the second medium as shown in Figure 2.2. In other words, there is a slab between two half spaces and the object is located in the slab. The spaces are nonmagnetic, linear, isotropic, homogeneous and lossless. The object will be illuminated by planewaves having different incidence angle θ_i to collect scattered data along the measurement line shown in Figure 2.2.

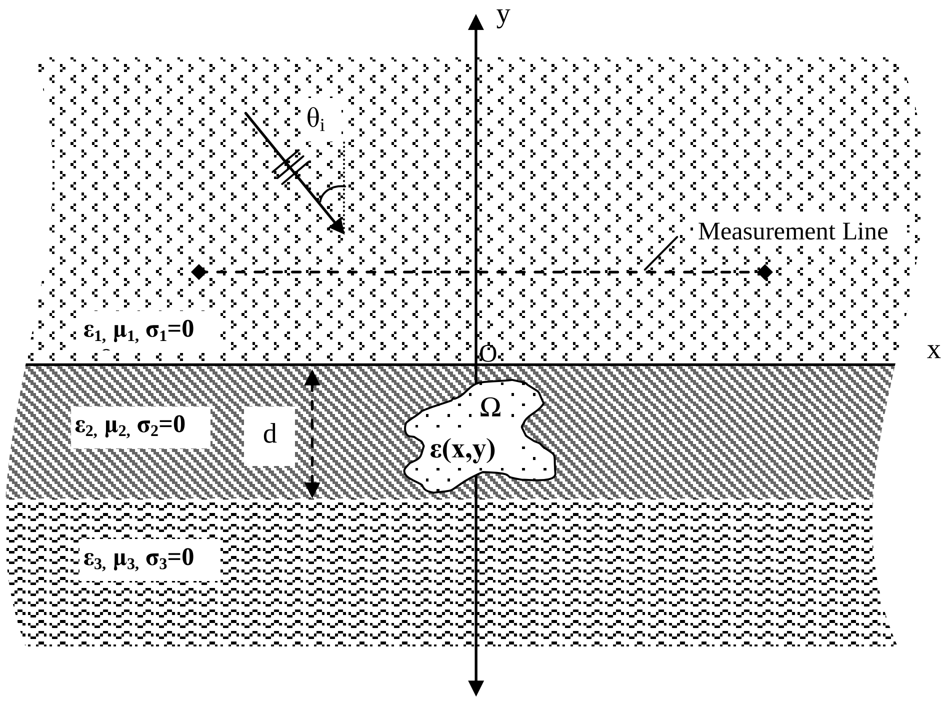

Figure 2.2 : The problem geometry for the forward problem.

The solution procedure for the forward problem was depicted in Section 2.1. The Green's functions pertaining to three part planarly layered media can be employed to apply MOM solution. The Green's function satisfies (2.21).

$$\Delta G(x,y;x',y') + k^2(y) \cdot G(x,y;x',y') = -\delta(x-x') \cdot \delta(y-y') \qquad \textbf{(2.21)}$$

where

$$k(y) = \begin{cases} k_1, & y > 0 \\ k_2, & -d < y < 0 \\ k_3, & y < -d \end{cases} \qquad \textbf{(2.22)}$$

$G(x,y;x',y')$ and $\frac{\partial G(x,y;x',y')}{\partial n}$ are continuous on the boundaries separating the media. There are different approaches to solve (2.21). One method, called hybrid method, suggests Fourier transform in one dimension and direct solution in other dimension [8]. We will perform Fourier transform over the horizontal axis and employ direct solution in the stratified direction. We apply Fourier transform to the whole equation given in (2.21).

$$\int_{-\infty}^{\infty} [\Delta G + k^2 \cdot G = -\delta(x-x') \cdot \delta(y-y')] \cdot e^{-i \cdot \nu \cdot x} \cdot dx \qquad \textbf{(2.23)}$$

using radiation condition

$$\frac{\partial \hat{G}}{\partial y} - \gamma_j \cdot \hat{G} = -e^{-i \cdot v \cdot x'} \cdot \delta(y - y') \qquad \textbf{(2.24)}$$

where $\hat{G}$stands for the spectral Green's function and

$$\gamma_j(v) = \sqrt{v^2 - {k_j}^2} \quad , \qquad j = 1, 2, 3 \qquad \textbf{(2.25)}$$

γ_j is defined with the condition $\gamma_j(0) = -i \cdot k_j$ in accordance with the complex cut plane as shown in Figure 2.3 [9].

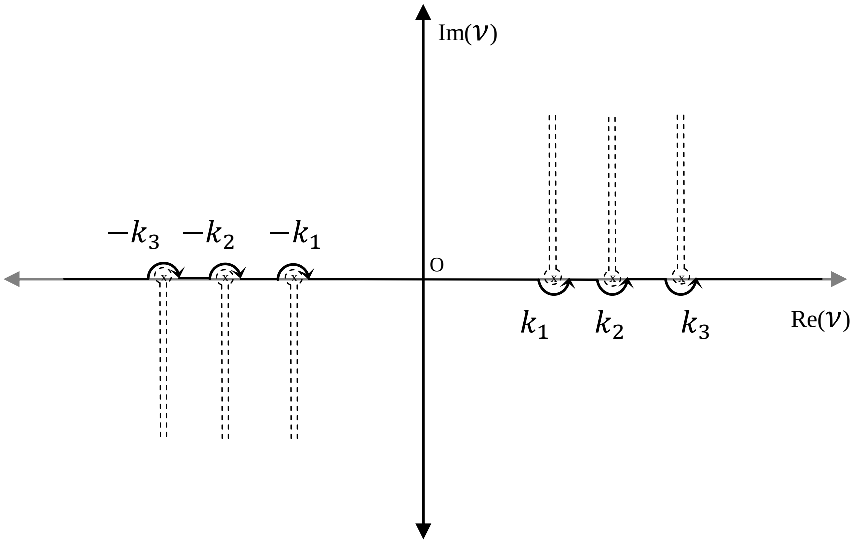

Figure 2.3 : Branch cuts and Fourier inversion path in the complex plane.

Nine solutions arise for (2.24) depending on which medium the source and the observation point are located in. These are the Green's functions named as from G_{11} to G_{33}. In each of nine case, system of linear equations consisting of eight unknowns and eight equations emerge. Six equations coming from Dirichlet and Neumann type conditions on boundaries and the source point, two equations imposed by radiation conditions form eight equations. Green's functions pertaining to three part planarly layered media is studied well in [10], only the components of G_{21}, G_{22} are dealt with in this work. They are given in (2.26) and (2.27)

$$G_{21}(x, y; x', y') = \int_{FIP} e^{-\gamma_1 \cdot y + \gamma_2 \cdot y'} \cdot C_{211} \cdot e^{i \cdot v \cdot (x - x')} \cdot dv \qquad \textbf{(2.26)}$$

$$+ \int_{FIP} e^{-\gamma_1 \cdot y - \gamma_2 \cdot y'} \cdot C_{212} \cdot e^{i \cdot \nu \cdot (x - x')} \cdot d\nu$$

$$G_{22}(x, y; x', y') = \frac{i}{4} \cdot H_0^{(1)} \left(k_2 \cdot \sqrt{(x - x')^2 + (y - y')^2} \right)$$

$$+ \int_{FIP} e^{\gamma_2 \cdot (y + y')} \cdot C_{221} \cdot e^{i \cdot \nu \cdot (x - x')} \cdot d\nu$$

$$+ \int_{FIP} e^{-\gamma_2 \cdot (y + y')} \cdot C_{222} \cdot e^{i \cdot \nu \cdot (x - x')} \cdot d\nu \tag{2.27}$$

$$+ \int_{FIP} e^{\gamma_2 \cdot (y' - y)} \cdot C_{223} \cdot e^{i \cdot \nu \cdot (x - x')} \cdot d\nu$$

$$+ \int_{FIP} e^{\gamma_2 \cdot (y - y')} \cdot C_{224} \cdot e^{i \cdot \nu \cdot (x - x')} \cdot d\nu$$

where FIP stands for Fourier inversion path. The coefficients are given by (2.28)-(2.34) [10].

$$C_{211} = \frac{1}{2\pi} \cdot \frac{e^{2 \cdot \gamma_2 \cdot \mathrm{d}} \cdot (\gamma_3 + \gamma_2)}{P} \tag{2.28}$$

$$C_{212} = \frac{1}{2\pi} \cdot \frac{(\gamma_2 - \gamma_3)}{P} \tag{2.29}$$

$$C_{221} = \frac{1}{2\pi} \cdot \frac{1}{2 \cdot \gamma_2} \cdot \frac{e^{2 \cdot \gamma_2 \cdot \mathrm{d}} \cdot (\gamma_3 + \gamma_2) \cdot (\gamma_2 - \gamma_1)}{P} \tag{2.30}$$

$$C_{222} = \frac{1}{2\pi} \cdot \frac{1}{2 \cdot \gamma_2} \cdot \frac{(\gamma_2 - \gamma_3) \cdot (\gamma_2 + \gamma_1)}{P} \tag{2.31}$$

$$C_{223} = \frac{1}{2\pi} \cdot \frac{1}{2 \cdot \gamma_2} \cdot \frac{(\gamma_2 - \gamma_3) \cdot (\gamma_2 - \gamma_1)}{P} \tag{2.32}$$

$$C_{224} = C_{223} \tag{2.33}$$

$$P = e^{2\cdot\gamma_2\cdot d}\cdot(\gamma_3+\gamma_2)\cdot(\gamma_2+\gamma_1)+(\gamma_2-\gamma_3)\cdot(\gamma_2-\gamma_1) \quad \textbf{(2.34)}$$

One should calculate surface integrals of the Green's functions over a cell area to fill the matrix C. Cell size in x is Δx and in y is Δy, (x_c, y_c) holds center coordinates of the cells. Surface integrals of the Green's functions can be calculated as follows.

$$\int_{y_c-\frac{\Delta y}{2}}^{y_c+\frac{\Delta y}{2}}\int_{x_c-\frac{\Delta x}{2}}^{x_c+\frac{\Delta x}{2}} G_{21}(x,y;x',y')\cdot dx'dy' =$$

$$C_{211}\cdot\int_{FIP} e^{\gamma_2\cdot(y+y')}\cdot e^{i\cdot v\cdot(x-x_c)}\cdot\frac{4\cdot\sin(\Delta x\cdot v/2)\cdot\sinh(\Delta y\cdot\gamma_2/2)}{\gamma_2\cdot v}\cdot dv \quad \textbf{(2.35)}$$

$$+\ C_{212}\int_{FIP} e^{-\gamma_1\cdot y-\gamma_2\cdot y_c}\cdot e^{i\cdot v\cdot(x-x_c)}\cdot\frac{4\cdot\sin(\Delta x\cdot v/2)\cdot\sinh(\Delta y\cdot\gamma_2/2)}{\gamma_2\cdot v}\cdot dv$$

$$\int_{y_c-\frac{\Delta y}{2}}^{y_c+\frac{\Delta y}{2}}\int_{x_c-\frac{\Delta x}{2}}^{x_c+\frac{\Delta x}{2}} G_{22}(x,y;x',y')\cdot dx'dy'$$

$$= \begin{cases} \dfrac{i\cdot\pi\cdot a}{2\cdot k_2}\cdot H_1^{(1)}(k_2\cdot a)-\dfrac{1}{{k_2}^2}, & x=x' \wedge y=y' \\ \dfrac{i\cdot\pi\cdot a}{2\cdot k_2}\cdot J_1\ (k_2\cdot a)H_0^{(1)}\left(k_2\cdot\sqrt{(x-x')^2+(y-y')^2}\right), & otherwise \end{cases}$$

$$+C_{221}\cdot\int_{FIP} e^{\gamma_2\cdot(y+y')}\cdot e^{i\cdot v\cdot(x-x_c)}\cdot 4\cdot\frac{\sin\left(\Delta x\cdot\frac{v}{2}\right)\cdot\sinh\left(\Delta y\cdot\frac{\gamma_2}{2}\right)}{\gamma_2\cdot v}\cdot dv \quad \textbf{(2.36)}$$

$$+C_{222}\cdot\int_{FIP} e^{-\gamma_2\cdot(y+y')}\cdot e^{i\cdot v\cdot(x-x_c)}\cdot 4\cdot\frac{\sin\left(\Delta x\cdot\frac{v}{2}\right)\cdot\sinh\left(\Delta y\cdot\frac{\gamma_2}{2}\right)}{\gamma_2\cdot v}\cdot dv$$

$$+C_{223}\cdot\int_{FIP} e^{\gamma_2\cdot(y_c-y)}\cdot e^{i\cdot v\cdot(x-x_c)}\cdot 4\cdot\frac{\sin\left(\Delta x\cdot\frac{v}{2}\right)\cdot\sinh\left(\Delta y\cdot\frac{\gamma_2}{2}\right)}{\gamma_2\cdot v}\cdot dv$$

$$+C_{224}\int_{FIP} e^{-\gamma_2\cdot(y_c-y)}\cdot e^{i\cdot v\cdot(x-x_c)}\cdot 4\cdot\frac{\sin(\Delta x\cdot v/2)\cdot\sinh(\Delta y\cdot\gamma_2/2)}{\gamma_2\cdot v}\cdot dv$$

Numerical calculations has shown that surface integrals can be approximated by multiplication of the integrand and the cell area. It is seen that when the cell size is kept small enough, incurred error is acceptable.

Now, only the incident field is left to be determined. The incident field can be calculated as follows.

One can write components of electric and magnetic fields in each region as shown in Figure 2.4. Then, corresponding boundary conditions can be imposed.

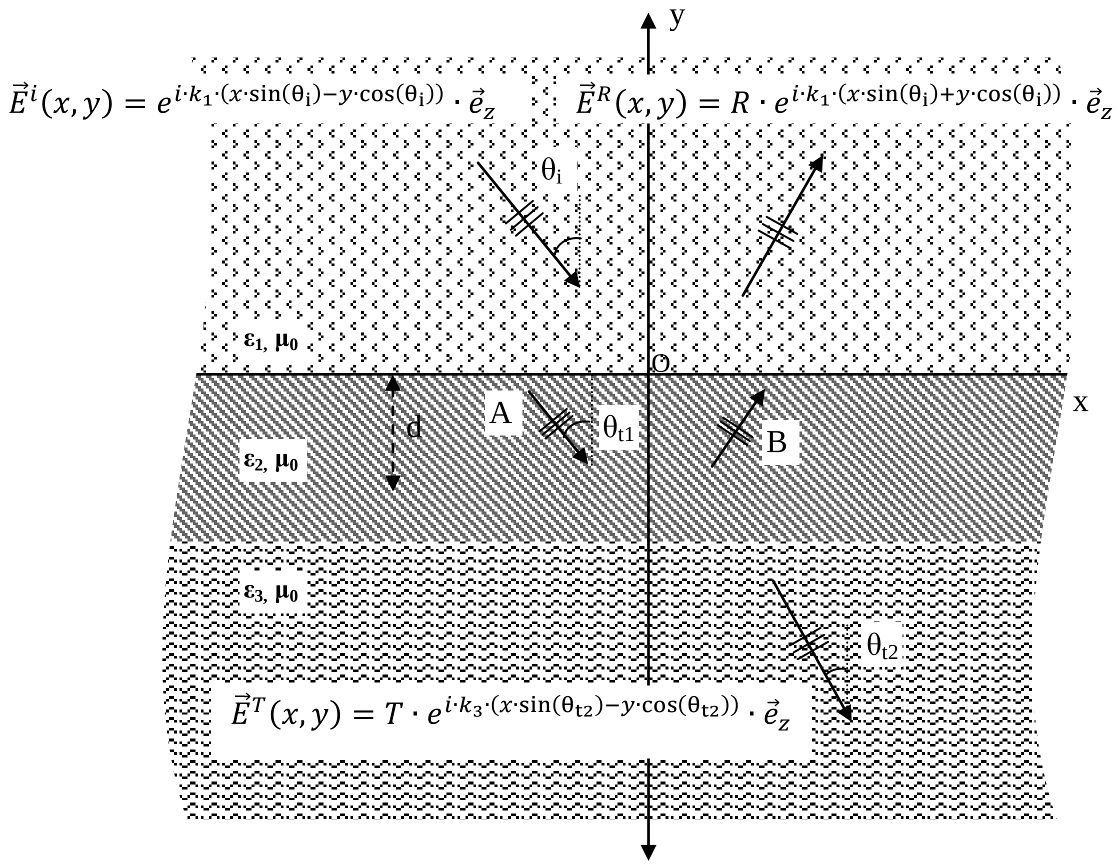

Figure 2.4 : Calculation of the incident field.

The electric and the magnetic fields in the upper half space are given in (2.37) and (2.38).

$$\vec{E}^i(x,y) = e^{i\cdot k_1\cdot(x\cdot\sin(\theta_i)-y\cdot\cos(\theta_i))}\cdot\vec{e}_z \qquad \textbf{(2.37)}$$

$$\vec{H}^i(x,y) = \frac{1}{\eta_1}\cdot e^{i\cdot k_1\cdot(x\cdot\sin(\theta_i)-y\cdot\cos(\theta_i))}\cdot(-\vec{e}_y\cdot\sin(\theta_i)-\vec{e}_x\cdot\cos(\theta_i)) \qquad \textbf{(2.38)}$$

In slab, the field components are given in (2.39) and (2.40).

$$\vec{E}^S(x,y) = A \cdot e^{i\cdot k_2\cdot(x\cdot\sin(\theta_{t1})-y\cdot\cos(\theta_{t1}))} \cdot \vec{e}_z + B \cdot e^{i\cdot k_2\cdot(x\cdot\sin(\theta_{t1})+y\cdot\cos(\theta_{t1}))} \cdot \vec{e}_z \quad \mathbf{(2.39)}$$

$$\vec{H}^S(x,y) = A \cdot \frac{1}{\eta_2} \cdot e^{i\cdot k_2\cdot(x\cdot\sin(\theta_{t1})-y\cdot\cos(\theta_{t1}))} \cdot (-\vec{e}_y \cdot \sin(\theta_i) - \vec{e}_x \cdot \cos(\theta_i)) + B \cdot \frac{1}{\eta_2} \cdot e^{i\cdot k_2\cdot(x\cdot\sin(\theta_{t1})+y\cdot\cos(\theta_{t1}))} \cdot (-\vec{e}_y \cdot \sin(\theta_i) + \vec{e}_x \cdot \cos(\theta_i)) \quad \mathbf{(2.40)}$$

In the lower half space, the field components are given in (2.41) and (2.42).

$$\vec{E}^T(x,y) = T \cdot e^{i\cdot k_3\cdot(x\cdot\sin(\theta_{t2})-y\cdot\cos(\theta_{t2}))} \cdot \vec{e}_z \quad \mathbf{(2.41)}$$

$$\vec{H}^T(x,y) = \frac{1}{\eta_3} \cdot T \cdot e^{i\cdot k_3\cdot(x\cdot\sin(\theta_{t2})-y\cdot\cos(\theta_{t2}))} \cdot (-\vec{e}_y \cdot \sin(\theta_{t2}) - \vec{e}_x \cdot \cos(\theta_{t2})) \quad \mathbf{(2.42)}$$

The boundary equations are imposed. Boundary equations at y=0 yields (2.43) and (2.44)

$$1 + R = A + B \quad \mathbf{(2.43)}$$

$$\frac{1}{\eta_1} \cdot -\cos(\theta_i) + \frac{1}{\eta_2} \cdot R \cdot \cos(\theta_i) = \frac{A}{\eta_2} \cdot -\cos(\theta_{t1}) + \frac{B}{\eta_2} \cdot \cos(\theta_{t1}) \quad \mathbf{(2.44)}$$

and at y=-d (2.45) and (2.46) can be written.

$$A \cdot e^{i\cdot k_2\cdot d\cdot\cos(\theta_{t1})} + B \cdot e^{i\cdot k_2\cdot -d\cdot\cos(\theta_{t1})} = T \cdot e^{i\cdot k_3\cdot d\cdot\cos(\theta_{t2})} \quad \mathbf{(2.45)}$$

$$\frac{A}{\eta_2} \cdot e^{i\cdot k_2\cdot d\cdot\cos(\theta_{t1})} \cdot -\cos(\theta_{t1}) + \frac{B}{\eta_2} \cdot e^{i\cdot k_2\cdot -d\cdot\cos(\theta_{t1})} \cdot \cos(\theta_{t1}) = \frac{T}{\eta_3} \cdot e^{i\cdot k_3\cdot d\cdot\cos(\theta_{t2})} \cdot -\cos(\theta_{t2}) \quad \mathbf{(2.46)}$$

The diffraction angles θ_{t1} and θ_{t2} can be found using the well-known Snell's law given in (2.47).

$$k_1 \cdot \sin(\theta_\mathrm{i}) = k_2 \cdot \sin(\theta_{\mathrm{t}1}) = k_3 \cdot \sin(\theta_{\mathrm{t}2}) \qquad \textbf{(2.47)}$$

Equations from (2.43) to (2.46) form a system of linear equations, the coefficients R, A, B and T can be found easily by filling a 4x4 matrix in a CAD tool. Recursive formulas for the reflection and transmission coefficients for a multilayer planarly layered media can be found in [11].

The C matrix is filled and the incident field vector E^i is calculated. The matrix equation (2.17) can be solved for the unknown electric field variable by inverting the matrix C. As it is mentioned in Section 2.1; once the electric field is found, scattered data can be produced via (2.19).

3. NUMERICAL RESULTS AND COMMENTS FOR THE FORWARD PROBLEMS

The ultimate goal of the work is to solve an inverse problem. The forward problem is solved in order to provide data to the inverse problem study. It must be proved that the formulation of the forward problem and the produced scattering data are exactly correct so that the studies on the inversion algorithms are meaningful. Otherwise, it may be committed so-called inverse crime.

The best way to prove the results of the forward problem is to solve the forward problem with an entirely different numerical method and compare the results. It had been intended to solve the problem with FEM in addition to MOM. It is achieved to correctly model and produce scattered data for the forward problem for objects located in infinite medium in FEM. However, it is not the same for objects located in three part planarly layered media. The FEM solution in three part media is left as future work.

Nevertheless, the following results are powerful evidences indicating the forward solution is correct.

It is checked first that whether the spectral representation of the Hankel function can be computed over FIP correctly. The magnitudes and the phases are compared and results are shown in Figure 3.1 and Figure 3.2.

$$\frac{i}{4} \cdot H_0^{(1)}\left(k_1 \cdot \sqrt{(x-x')^2+(y-y')^2}\right) = \frac{1}{2\pi} \cdot \int_{FIP} \frac{1}{2\gamma_1} \cdot e^{\gamma_1 \cdot |y-y'|} \cdot e^{i \cdot v \cdot (x-x')} \cdot dv \qquad \textbf{(3.1)}$$

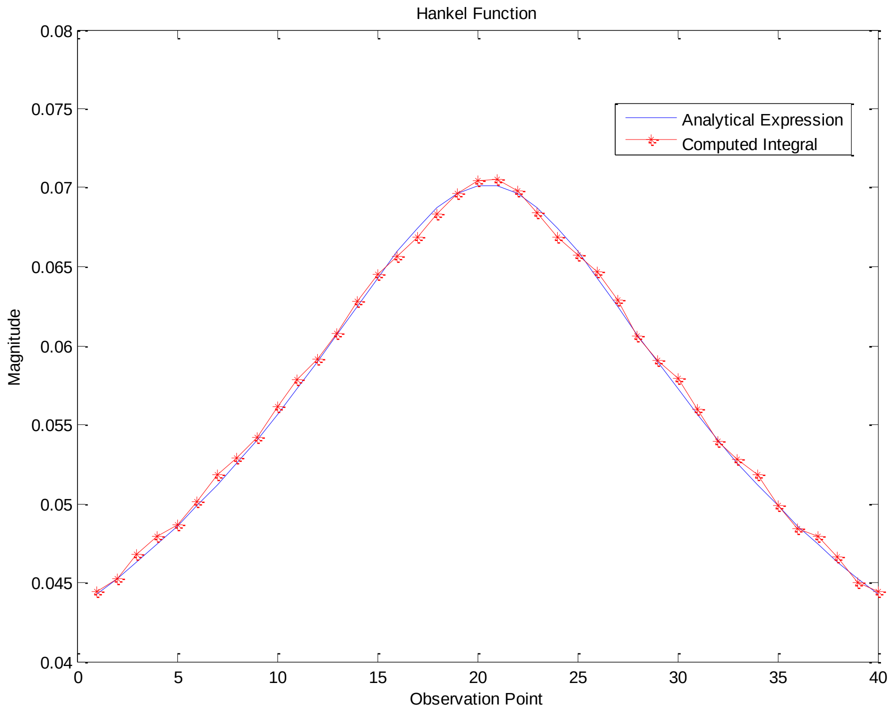

Figure 3.1 : Magnitude of the Hankel function, analytical and computed.

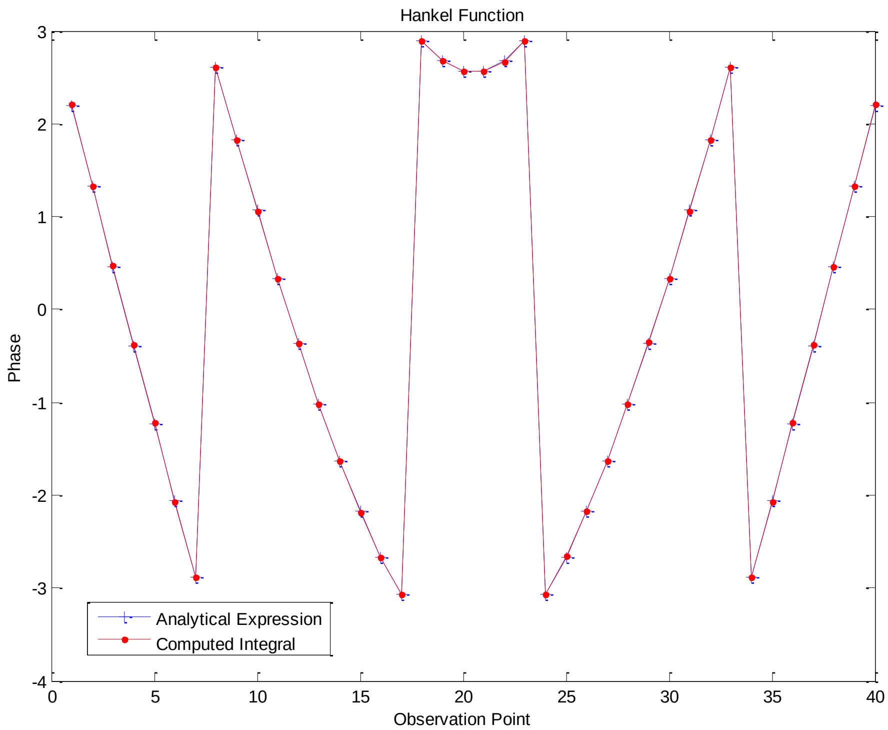

Figure 3.2 : Phase of the Hankel function, analytical and computed.

Then, electrical properties of three mediums are chosen the same as shown in Figure 3.3 in order to check forward solution results against to analytical expressions and FEM solution also. Results are given in Figure 3.4 and Figure 3.5.

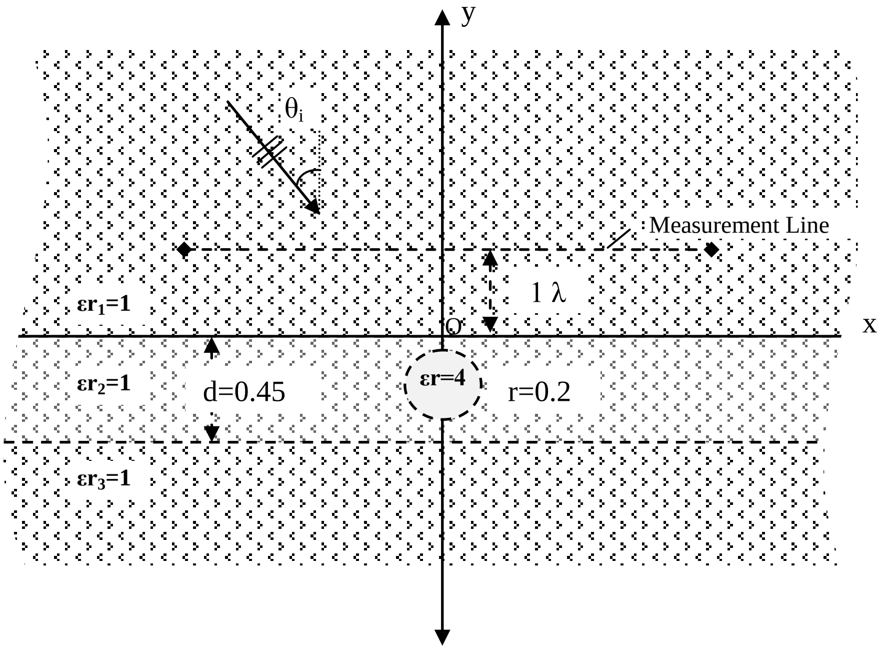

Figure 3.3 : Forward solution check geometry.

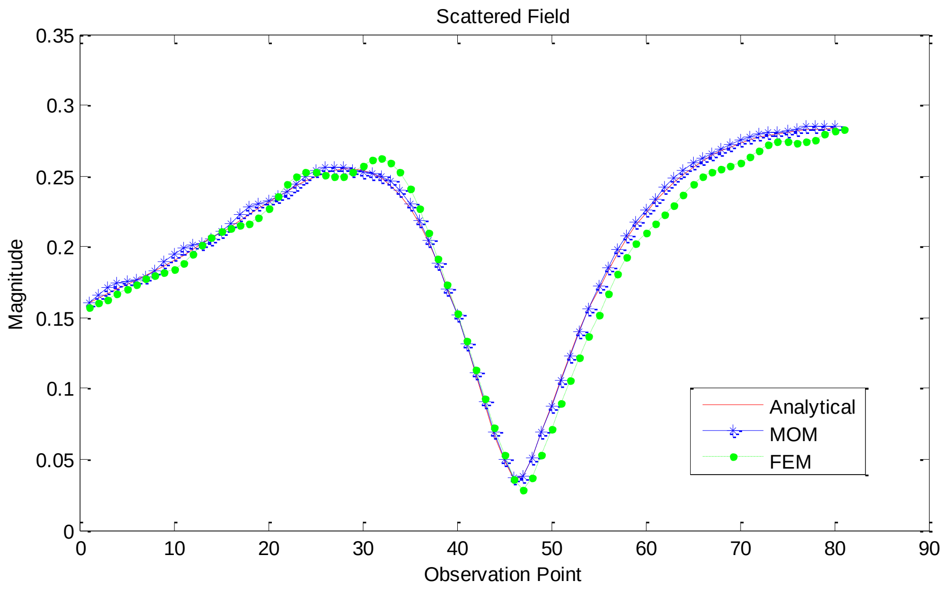

Figure 3.4 : Comparison of scattered fields for incidence angle of pi/4.

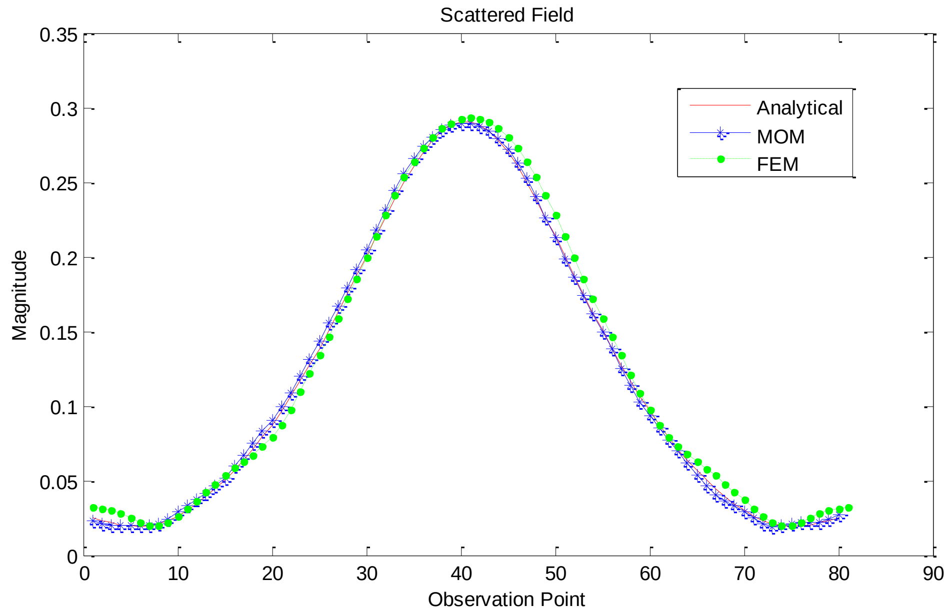

Figure 3.5 : Comparison of scattered fields for normal incidence.

Although the forward solution could not be modeled in an entirely different numerical method, according to obtained results there is nothing looking wrong in the forward solution.

4. INVERSE PROBLEMS FOR OBJECTS LOCATED IN THREE PART PLANARLY LAYERED MEDIA

The inverse scattering problem is determination of contrast of the scatterer object(s) from knowledge of the incident and the scattered fields. Once the contrast of the scatterer immersed in a known background is determined, its both electrical and geometrical properties are determined because the contrast function, by definition, holds the both properties.

The inverse problems are generally nonlinear and highly ill-posed. Existence of a unique solution of an inverse problem is also a research topic.

4.1 The Problem Geometry for the Inverse Problem

The problem is a two dimensional problem and the geometry consists of three part planarly layered media. The scattering object(s) is located in the second medium in a hypothetical, square reconstruction domain D. The problem geometry is shown in Figure 4.1. The spaces are homogeneous, nonmagnetic and lossless i.e. $\mu_1 = \mu_2 = \mu_3 = \mu_0$ and $\sigma_1 = \sigma_2 = \sigma_3 = 0$.

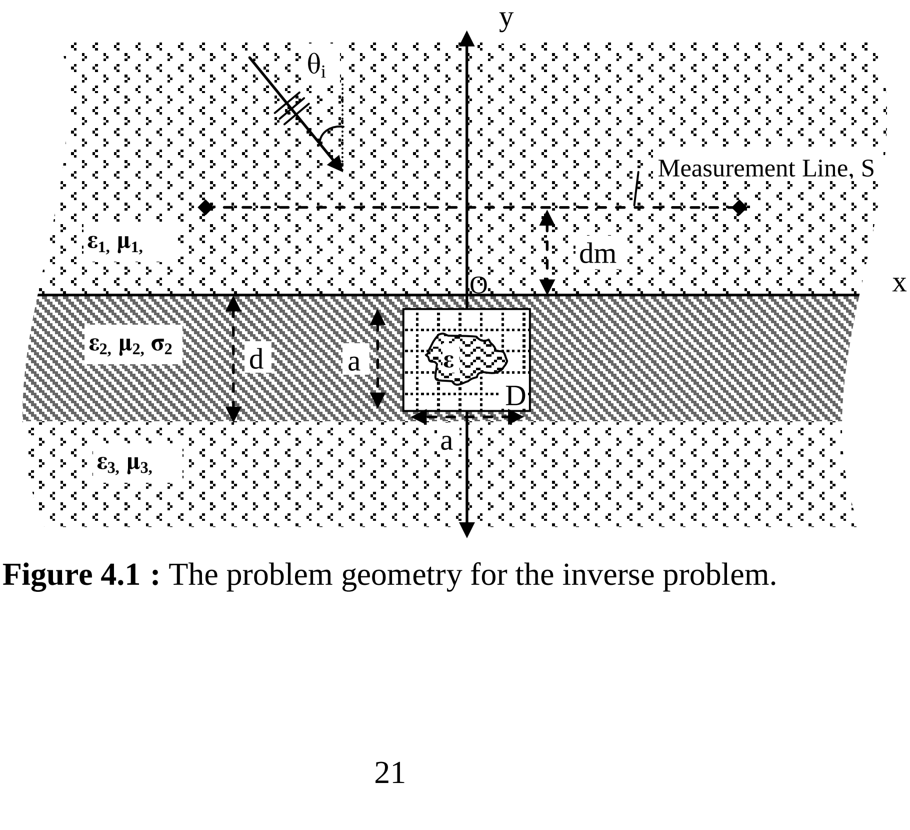

Figure 4.1 : The problem geometry for the inverse problem.

The following parameters are used for the shown geometry throughout the thesis unless otherwise noted.

Thickness of the slab, $d = 0.45 \cdot \lambda_2$

Size of the reconstruction domain D, $a = 0.4 \cdot \lambda_2$

Distance of the measurement line S, $dm = 1 \cdot \lambda_1$

Dielectric constants of the media, $\boldsymbol{\varepsilon_1} = 1 \cdot \boldsymbol{\varepsilon}_0$, $\boldsymbol{\varepsilon_2} = 3 \cdot \boldsymbol{\varepsilon}_0$ and $\boldsymbol{\varepsilon_3} = 5 \cdot \boldsymbol{\varepsilon}_0$

The region is excited by plane waves having incidence angle $\theta_i$varying from $\frac{3\pi}{8}$ to $\frac{-3\pi}{8}$.

4.2 The Contrast Source Inversion Method

The contrast source inversion method is an algorithm for reconstruction of the contrast of a bounded object immersed in a known background medium. The method can employ both spatially and frequency varying incident fields and allows to introduce a priori information about the scatterer objects improving the reconstruction performance.

In this work, single frequency is used for the excitations and a priori information indicating the permittivity of the scattering object has no imaginary part and its real part is always positive is introduced. In other words, it is studied for the scattering objects whose dielectric constant are pure real and higher than the background medium.

It is known that total field in the domain D satisfies the domain integral equation

$$E(x,y) = E^i(x,y) + k^2 \int_{\mathrm{D}} \chi(x',y') \cdot E\,(x',y') \cdot G(x,y;x',y') \cdot dx' \cdot dy' \qquad \textbf{(4.1)}$$

and the scattered field data, on the measurement line S, can be found using (4.2).

$$E^s(x,y) = k^2 \int_{\mathrm{D}} \chi(x',y') \cdot E\,(x',y') \cdot G(x,y;x',y') \cdot dx' \cdot dy' \qquad \textbf{(4.2)}$$

The equations (4.1) and (4.2) are called state equation and data equation, respectively. They can be rewritten in a symbolic form. The state equation becomes (4.3)

$$E_j \quad = E_j^i + G_j^D(\chi_j \cdot E_j) \tag{4.3}$$

and the data equation becomes (4.4).

$$f_j \quad = G_j^S(\chi_j \cdot E_j) \tag{4.4}$$

The subscript j indicates excitation index and the operators $\mathrm{G^D}$ and $\mathrm{G^S}$ are defined implicitly in (4.1) and (4.2).

It is observed that the unknown variables χ and E appear as multiplication in the state and the data equation. The contrast source inversion method considers the multiplication of the mentioned variables as an equivalent source and names it *contrast source*.

$$w(x, y) = \chi(x, y) \cdot E(x, y) \tag{4.5}$$

The state and the data equation become (4.6) and (4.7).

$$E_j \quad = E_j^i + G_j^D(w_j) \tag{4.6}$$

$$f_j \quad = G_j^S(w_j) \tag{4.7}$$

The method handles the inverse problem as an optimization problem and aims to minimize a cost functional consisting of two terms pertaining to errors in the data equation and the object equation. The cost functional F is defined as in (4.8)

$$F = \frac{\sum_j ||\mathrm{\rho_j}||_S^2}{\sum_j ||f_j||_S^2} + \frac{\sum_j ||\mathrm{r_j}||_S^2}{\sum_j ||\chi_\mathrm{j} \cdot \mathrm{E_j^i}||_D^2} \tag{4.8}$$

where the data error and the state error defined in (4.9) and (4.10), respectively. $||.||_S^2$ and $||.||_D^2$ indicate norms on $L_2(S)$ and $L_2(D)$.

$$\mathrm{\rho_j} = f_j - \mathrm{G_j^s}(\mathrm{w_j}) \tag{4.9}$$

$$r_j = \chi_j \cdot E_j^i - w_j + \chi_j \cdot G_j^D(w_j) = \chi_j \cdot E_j \ \ - w_j \qquad \textbf{(4.10)}$$

The algorithm starts with initial values for the contrast source. There are two alternatives offered for the initial values, one consists of constant values minimizing the data error and the other is obtained by backpropagations. They are given in (4.11) and (4.12), respectively,

$$w_{j,0}^c = \frac{< f_j, G_j^s 1 >_S}{||G_j^s||_S^2} \qquad \textbf{(4.11)}$$

where $<.,.>_{S,D}$ stands for the inner product on L_2 [3].

$$w_{j,0}^{bp} = \frac{||G_j^{S^*} \cdot f_j||_D^2}{||G_j^S \ \ G_j^{S^*} \cdot f_j||_S^2} \cdot G_j^{S^*} \cdot f_j \qquad \textbf{(4.12)}$$

Second subscript of the contrast source in (4.11) and (4.12) indicates the iteration step so the value 0 indicates that the equations are initial assignment equations. The operators G^{S^*} and $G^{D^*}$are adjoints of G^S and G^D mapping from $L_2(S)$ to $L_2(D)$ and $L_2(D)$ to $L_2(D)$, respectively.

After the assignment of starting values, the algorithm constructs w and χ iteratively reducing the value of the cost functional in the following manner for n=0,1,2….

The contrast source is updated at each iteration step by the equation (4.13)

$$w_{j,n} = w_{j,n-1} + \alpha_{j,n} \cdot v_{j,n} \qquad \textbf{(4.13)}$$

where $\alpha_{j,n}$ is constants and $v_{j,n}$ is the Polak-Ribiere conjugate gradients update directions being function of the position. The initial value of the directions is zero.

$$v_{j,0} = 0 \qquad \textbf{(4.14)}$$

The update directions is given by (4.15)

$$v_{j,n} = g_{j,n} + \frac{< g_{j,n}, g_{j,n} - g_{j,n-1} >_D}{< g_{j,n-1}, g_{j,n-1} >_D} \cdot v_{j,n-1} \qquad \textbf{(4.15)}$$

where $g_{j,n}$ is Frechet derivative of the cost functional with respect to w_j evaluated at $w_{j,n-1}$ and $\chi_{j,n-1}$; $g_{j,n}$ is given by (4.16)

$$g_{j,n} = -\frac{G_j^{S^*}(\rho_{j,n-1})}{\sum_k ||f_k||_S^2} - \frac{r_{j,n-1} - G_j^{D^*}(\bar{\chi}_{j,n-1} \cdot r_{j,n-1})}{\sum_k ||\chi_{k,n-1} \cdot E_k^i||_D^2} \qquad \textbf{(4.16)}$$

and the constant $\alpha_{j,n}$ is determined to minimize the cost functional, it is given by (4.17) [3].

$$\alpha_{j,n} = \frac{\frac{<\rho_{j,n}, G_j^S v_{j,n}>_S}{\sum_k ||f_k||_S^2} + \frac{<r_{j,n-1}, v_{j,n} - \chi_{j,n-1} \cdot G_j^D v_{j,n}>_D}{\sum_k ||\chi_{k,n-1} \cdot E_k^i||_D^2}}{\frac{||G_j^S v_{j,n}||_S^2}{\sum_k ||f_k||_S^2} + \frac{||v_{j,n} - \chi_{j,n-1} \cdot G_j^D v_{j,n}||_D}{\sum_k ||\chi_{k,n-1} \cdot E_k^i||_D^2}} \qquad \textbf{(4.17)}$$

Once the $w_{j,n}$ is determined $u_{j,n}$ is determined using (4.18).

$$u_{j,n} = u_{j,n-1} + \alpha_{j,n} \cdot G_j^D\left(v_{j,n}\right) \qquad \textbf{(4.18)}$$

The application of the algorithm can be summarized by the following steps.

1) Determine start values using (4.12) or (4.12) for the contrast source.

2) Determine the Frechet derivative g and then determine update directions v.

3) Determine the constants α.

4) Update the contrast source w and then update the total field u.

5) Calculate contrast, χ.

6) Calculate the value of the cost functional, go Step 2 if it higher than specified error else go Step 7.

7) Exit from the loop and plot reconstructed contrast.

5. NUMERICAL RESULTS AND COMMENTS FOR THE INVERSE PROBLEMS

The method is applied for the objects located in an infinite medium first as the original paper depicts [3]. The geometry is shown in Figure 5.1. The reconstruction domain is 0.8λ x 0.8λ square and the measurement line is a circle having diameter of 1.6λ. The domain subdivided into square cells having size of λ/30. The region is illuminated by planewaves with 30 different incident angles being equally spaced in [0, 2π) and there are 30 measurement points on the measurement line. The excitation frequency is 3 GHz.

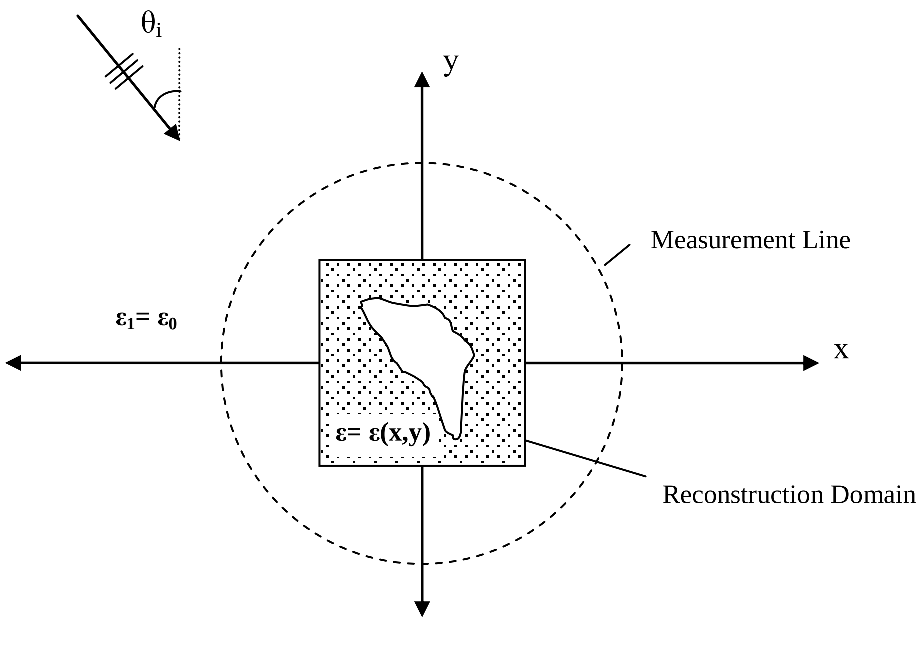

Figure 5.1 : An example geometry for the inverse problem.

The first example is circular cylinder whose radius is 0.2λ and contrast is 3.

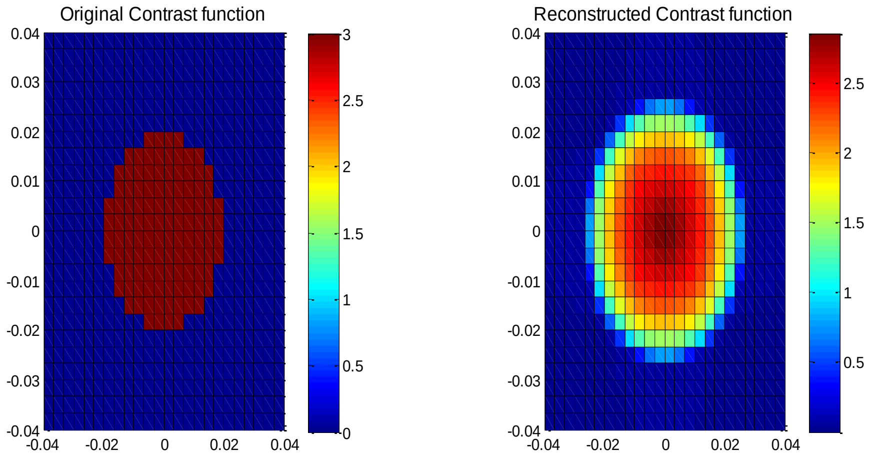

Figure 5.2 : A circular cylindrical object in infinite medium, original(left) reconstructed(right).

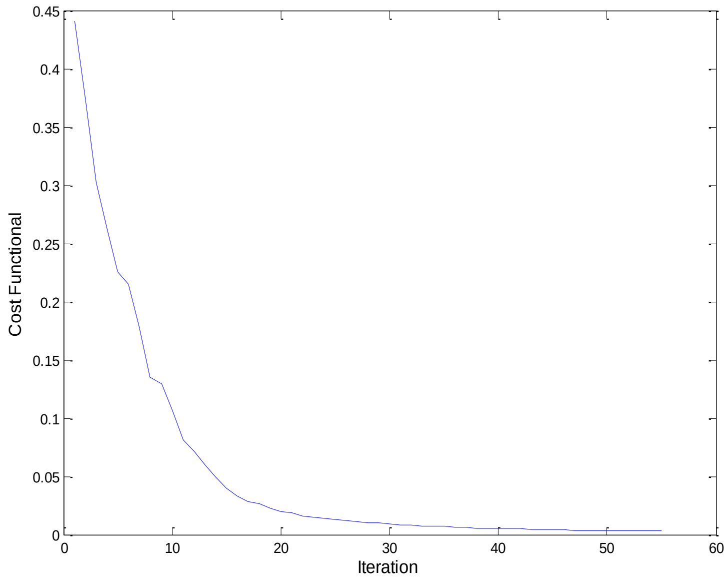

Figure 5.3 : Reconstruction of circular cylindrical object, cost functional vs iteration.

After 50 iterations the circular cylindrical object is reconstructed well. Then, a triangular object is tested as shown in Figure 5.4.

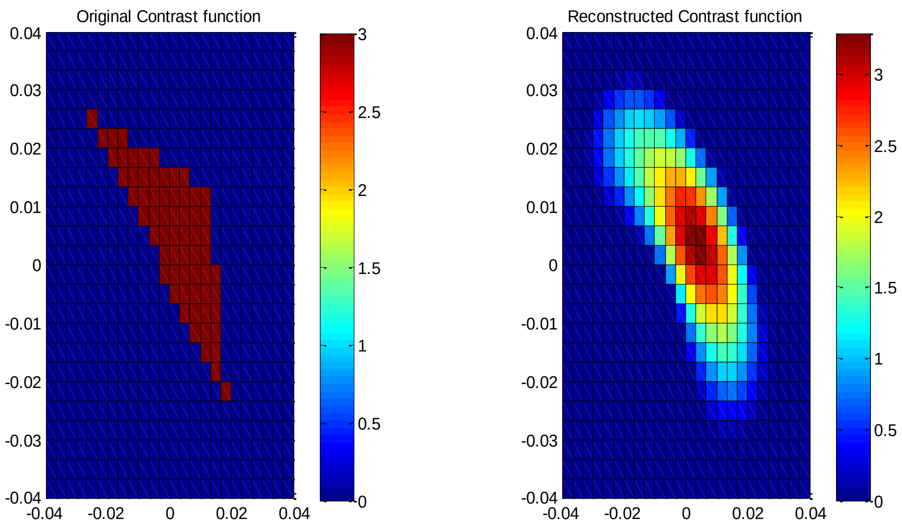

Figure 5.4 : Triangular cylindrical object in infinite medium.

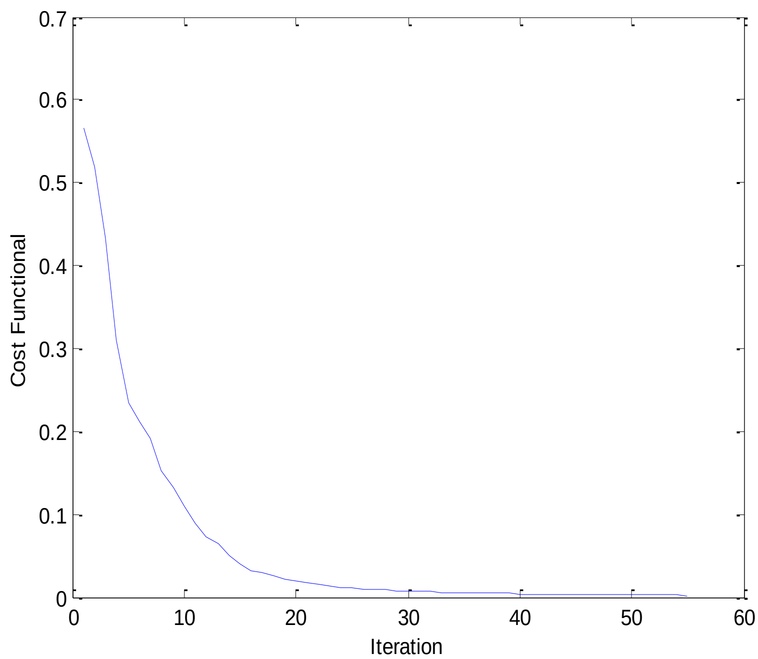

Figure 5.5 : Triangular cylindrical object cost functional vs iteration.

Two closely located objects are tested as shown in Figure 5.6.

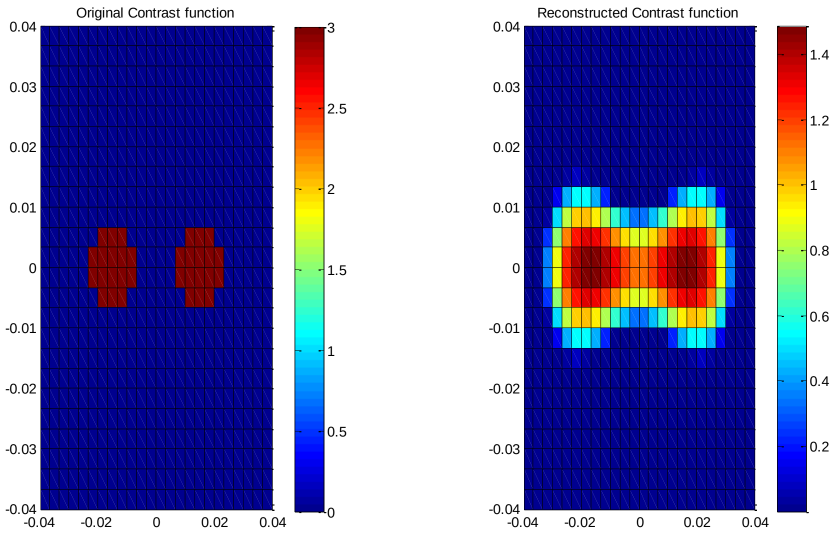

Figure 5.6 : Two objects separated by 0.3λ in infinite medium.

It can be seen in Figure 5.7 that objects having radius of less than 0.1λ can be clearly distinguished when they are separated by 0.4λ or more.

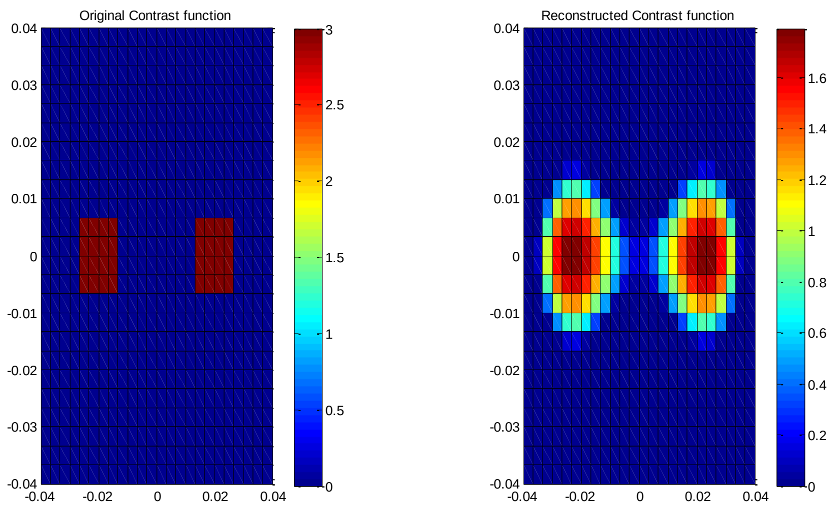

Figure 5.7 : Two objects separated by 0.4λ in infinite medium.

In Figure 5.8, it is seen that altering the objects' contrast does not disturb the reconstruction performance.

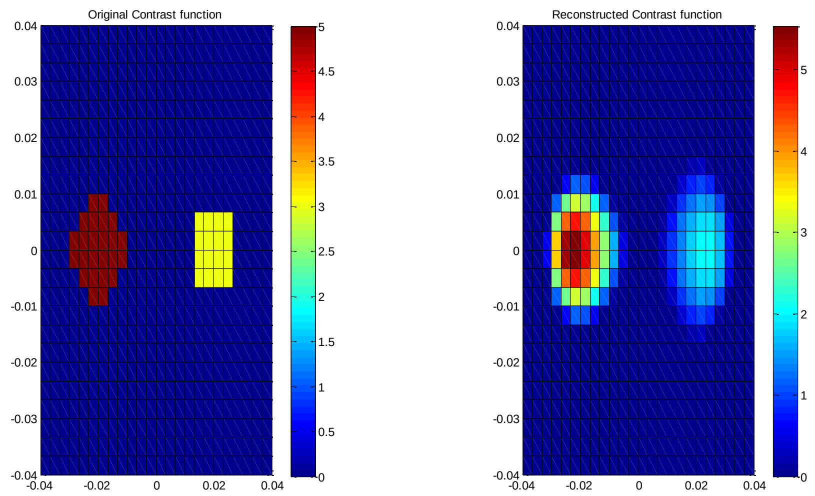

Figure 5.8 : Two objects with different contrasts are separated by 0.4λ in infinite medium.

In Figure 5.9, the object radius is less than 0.045 λ, although the contrast could not be found, the objects' location is detected.

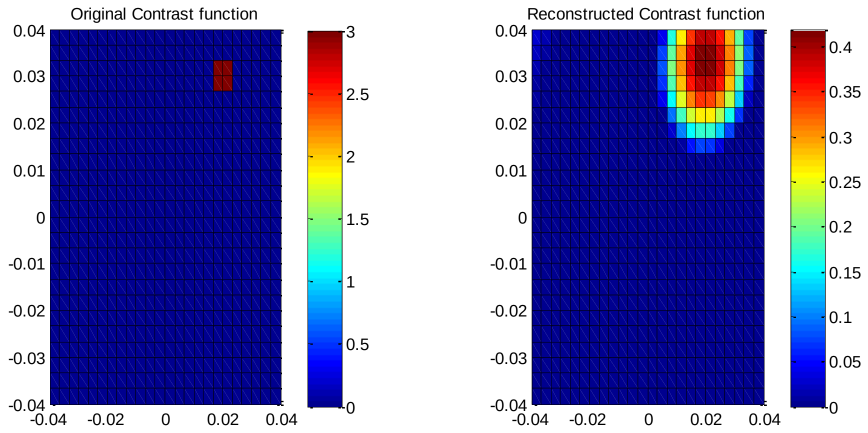

Figure 5.9 : Small off-centered object in infinite medium.

Then, the method is applied for the objects located in three part planarly layered media. The geometry was given in Figure 4.1. Following results are obtained for the objects located in three part planarly layered media.

In three part media, as it is mentioned, reconstruction domain is 0.4λ x 0.4λ and cell size is λ/30, λ indicates λ_2 throught the following results. The region is illuminated by planewaves with 80 different incident angles being equally spaced in [-3π/8, 3π/8)] and there are 80 measurement points on the measurement line. The excitation frequency is 3 GHz.

The first example is circular cylinder whose radius is 0.12λ and contrast is 3.

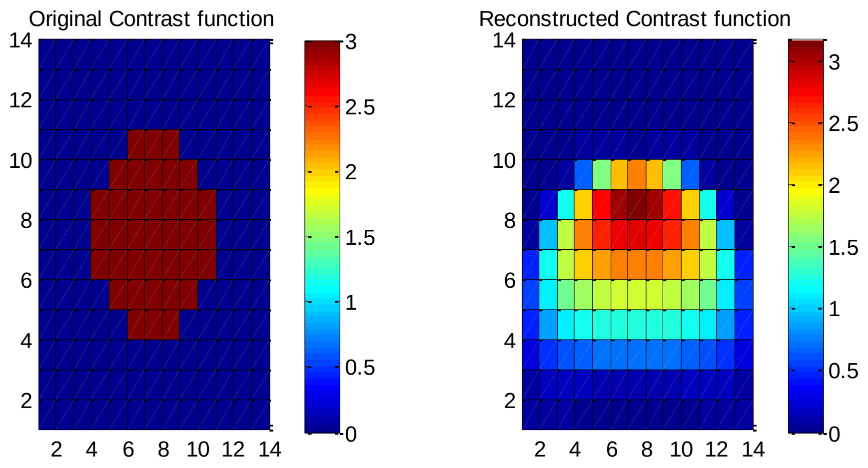

Figure 5.10 : Circular cylindrical object in stratified media, original(left) reconstructed(right).

Then, a triangular object is tested.

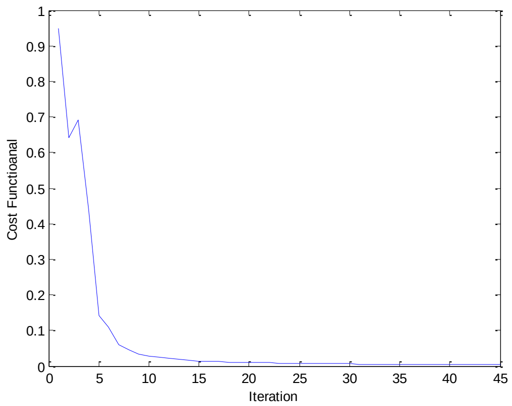

Figure 5.11 : Reconstruction of circular cylindrical object in stratified media, cost functional vs iteration.

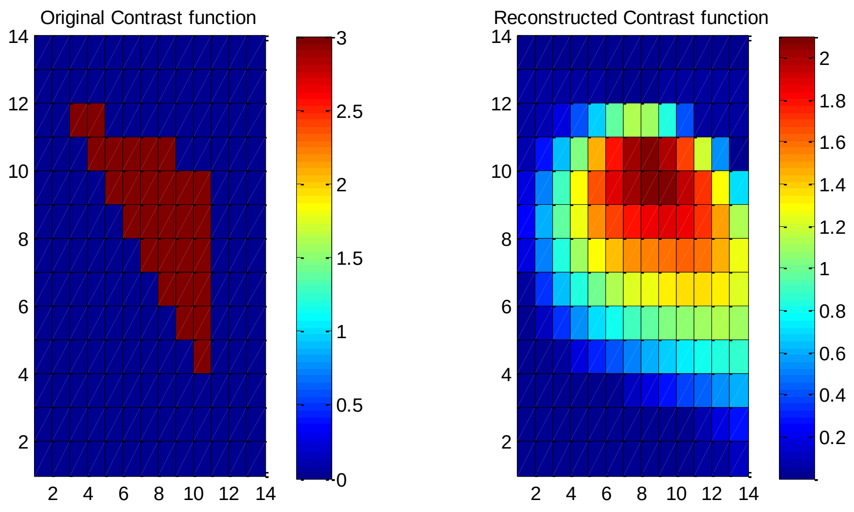

Figure 5.12 : Triangular cylindrical object in stratified media.

Reconstructed images smears down comparing to images obtained in infinite medium. This effect may be expected because the objects can only be illuminated by down going waves and scattered data can only be collected in upper half space.

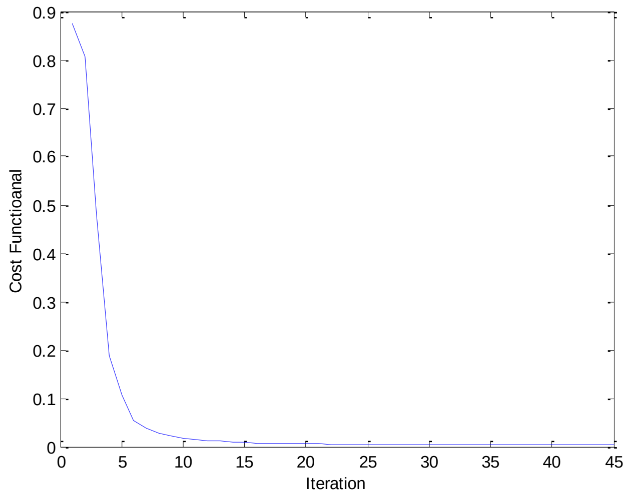

Figure 5.13 : Reconstruction of triangular cylindrical object in stratified media, cost functional vs iteration.

In Figure 5.14, it is seen that 0.2λ separated objects could not be reconstructed well; the bigger object is detected but the small object is disappeared at all. The bigger one has radius of 0.045λ and the small object's radius is 0.03λ.

When they are separated 0.3λ instead of 0.2λ and the radius of the small object is increased to 0.04λ, they can be distinguished as shown in Figure 5.15.

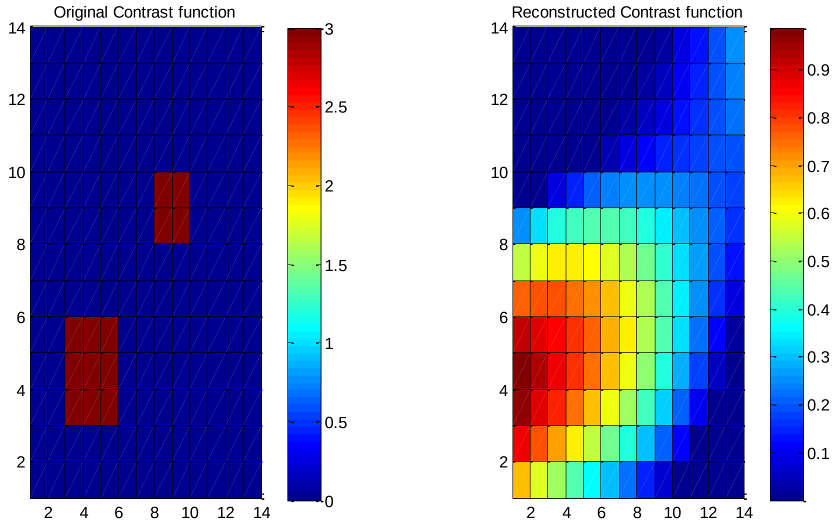

Figure 5.14 : Two objects separated by 0.2λ in stratified media.

The separation is kept 0.2λ and the reconstruction domain size is reduced to 0.3λ x 0.3λ to increase the resolution. The cell size is reduced to λ/40.

It is seen in Figure 5.16 that, none of the object is disappeared and they can be reconstructed better because the resolution is increased.

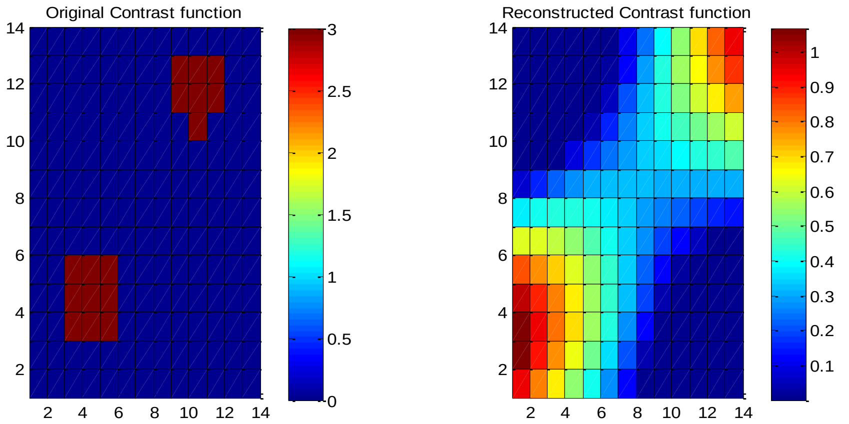

Figure 5.15 : Two objects separated by 0.3λ in stratified media.

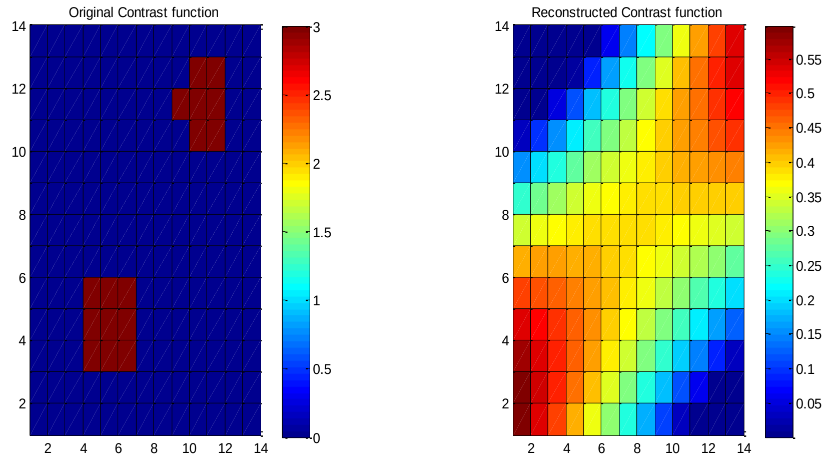

Figure 5.16 : Two objects separated by 0.2λ in stratified media, domain 0.3λ x 0.3λ.

In first example circular cylinder object having radius of 0.12λ was reconstructed well. When its radius is reduced 0.06λ, the result shown in Figure 5.17 is obtained.

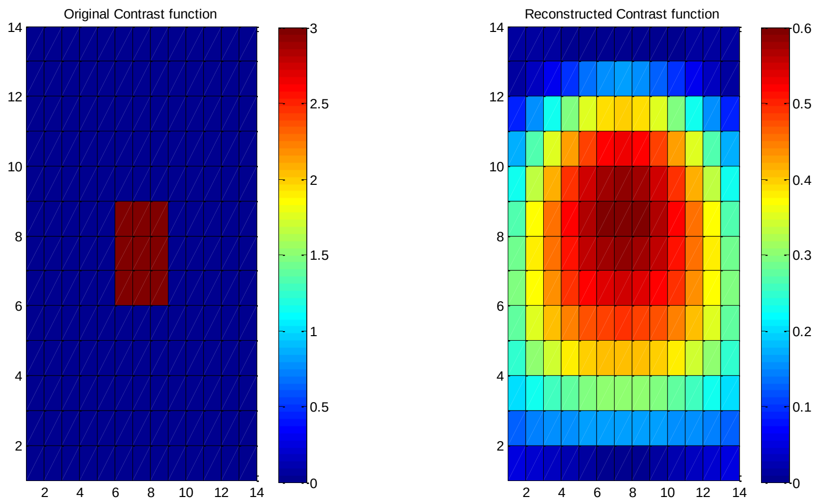

Figure 5.17 : Small object having radius of less than 0.06λ in stratified media.

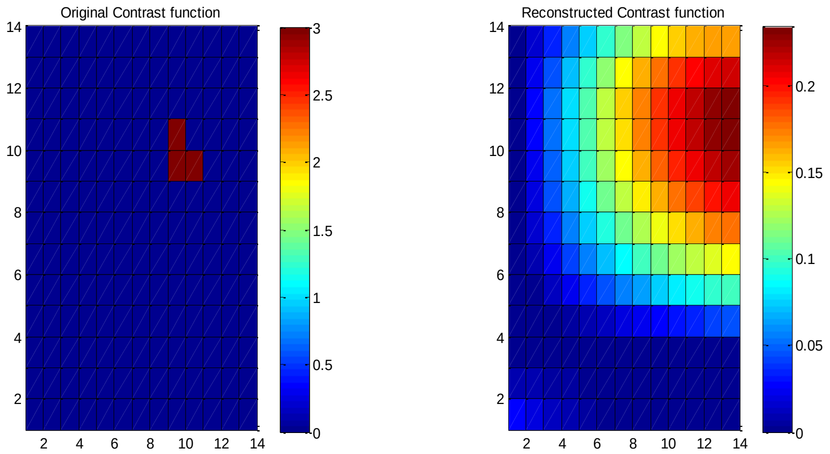

Figure 5.18 : Small off centered object having radius of less than 0.025λ in stratified media

It can be deduced from Figure 5.17 and Figure 5.18 that when the object radius goes below 0.1λ, although electrical properties can not be reconstructed well, their locations can be detected.

The slab thickness is increased to 0.65λ, reconstruction domain size is enlarged to 0.6λ x 0.6λ and cell size is reduced to λ/40 and following observations are carried out.

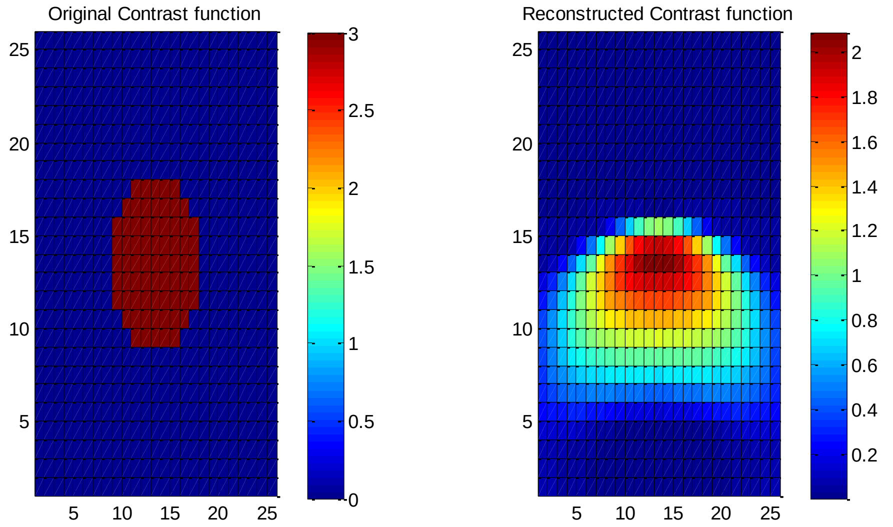

Figure 5.19 : Circular cylindrical object in stratified media, thick slab

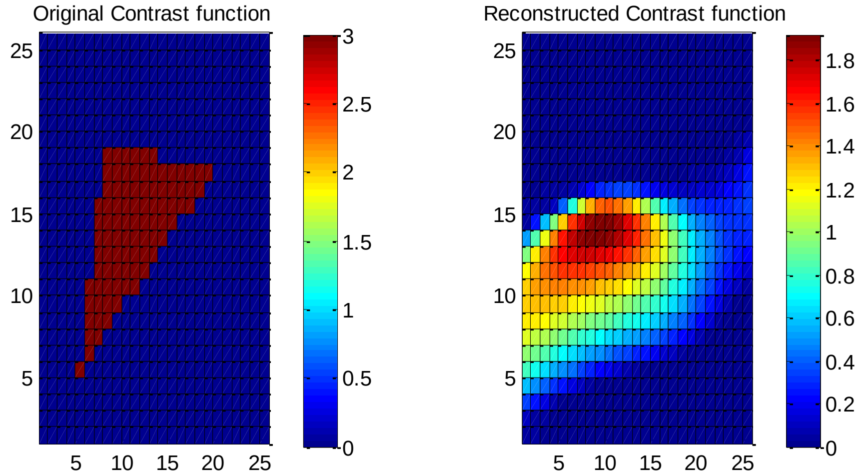

Figure 5.20 : Triangular cylindrical object in stratified media, thick slab

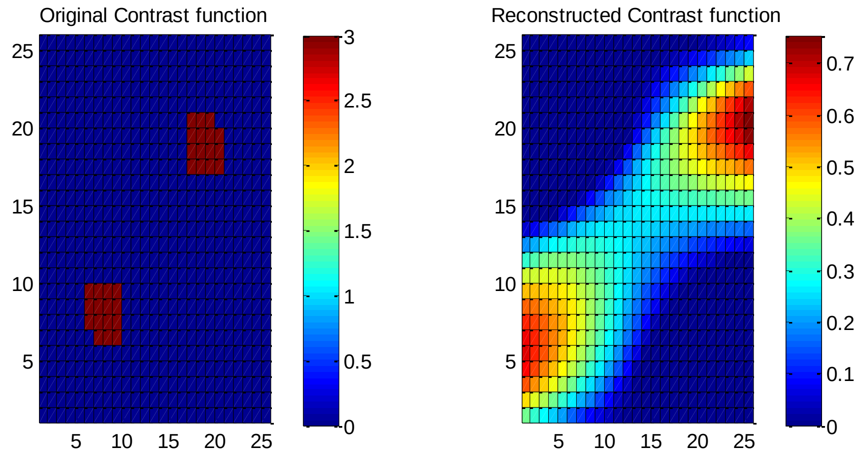

Figure 5.21 : Two objects in stratified media, separated, thick slab

Similar results are obtained for the thick slab (0.65λ). In two object case, objects can only be distinguished when they are get close to the opposite corners, otherwise one object overshadows the other object and their image become merged as seen from Figure 5.21 through Figure 5.23. When they are get closer to each other, they can not be separately reconstructed as shown in Figure 5.22.

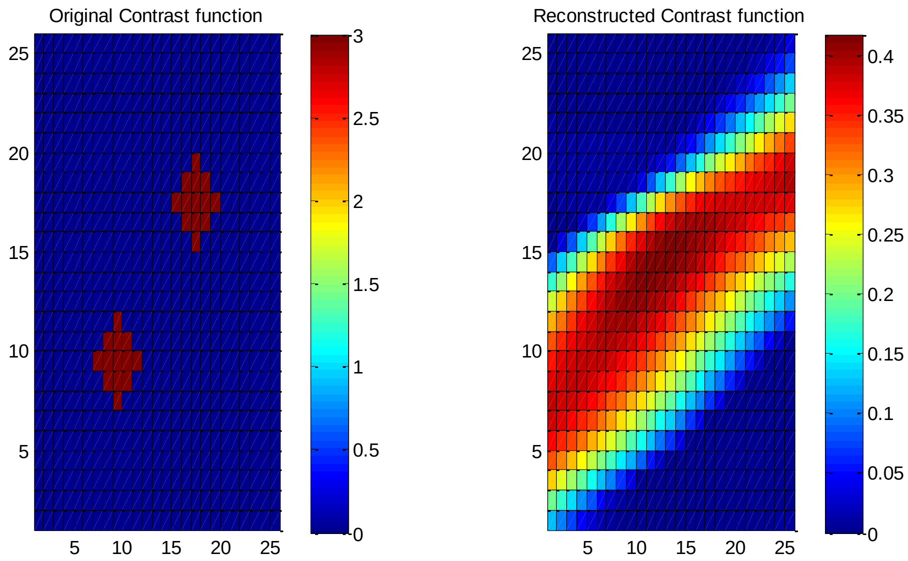

Figure 5.22 : Two objects in stratified media, merged, thick slab

The worst case is shown in Figure 5.23, one overshadows the other.

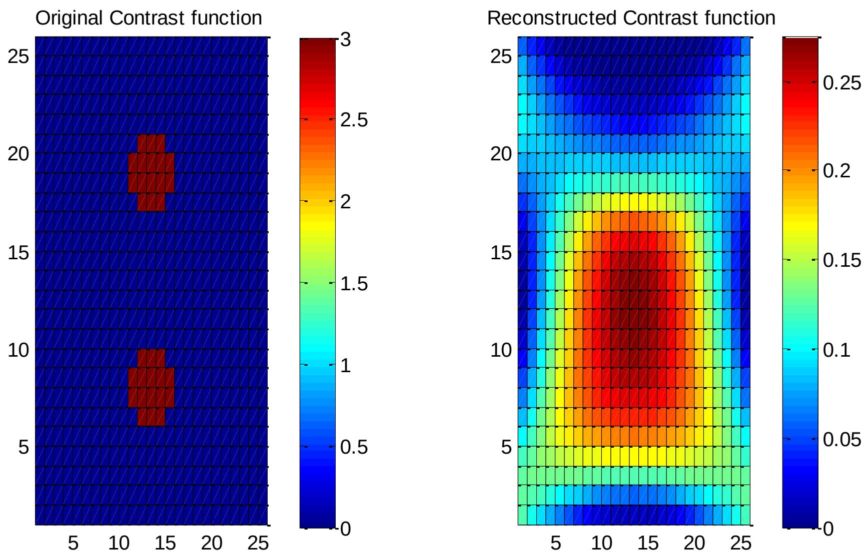

Figure 5.23 : Two objects in stratified media, worst case, thick slab

As a last study, reconstruction domain and cell size are kept the same, permittivity of the media changed as $\varepsilon_1 = 1 \cdot \varepsilon_0$, $\varepsilon_2 = 2 \cdot \varepsilon_0$ and $\varepsilon_3 = 7 \cdot \varepsilon_0$. It is observed for circular cylindrical object tests that the object's image may shift up or down with respect to its actual place according to its contrast. When the contrast get closer to the background's, image becomes shifted up and vice versa as show in Figure 5.24 through Figure 5.26.

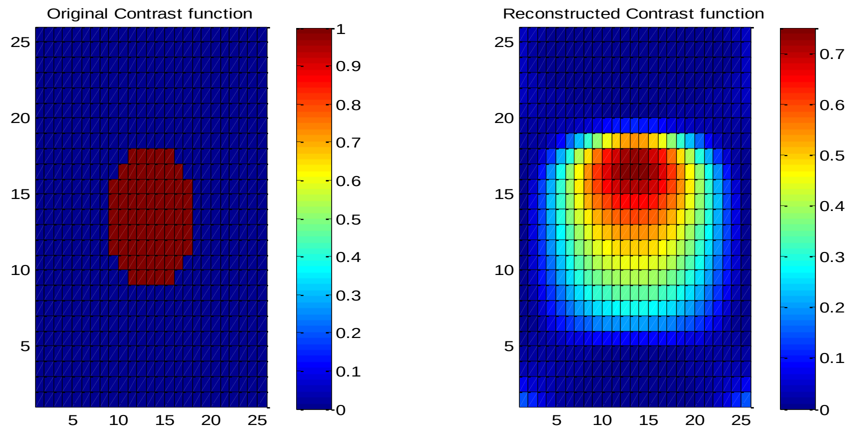

Figure 5.24 : Circular cylindrical object in stratified media, shifted up

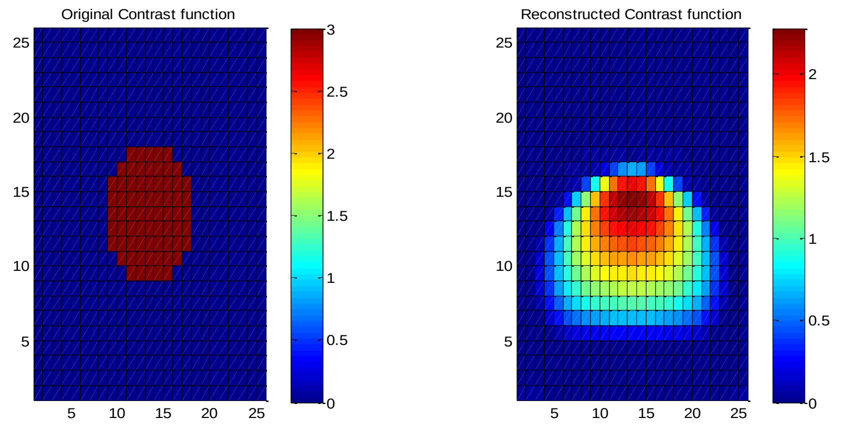

Figure 5.25 : Circular cylindrical object in stratified media, correct place

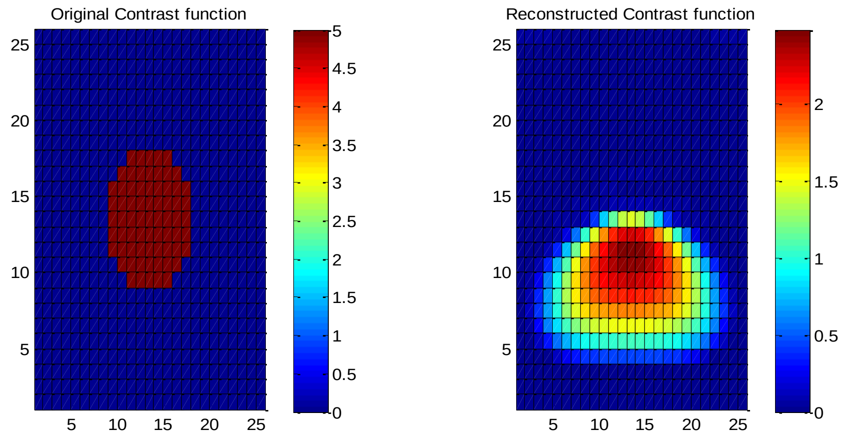

Figure 5.26 : Circular cylindrical object in stratified media, shifted down

As it is seen from the last three figures, contrast of the object affects the reconstruction performance. It can be deduced that for the objects having either much greater permittivity than background media or so close to the background media the reconstruction performance worsens. This behavior was also observed in previously examined cases, in the first case and in the thick slab case. In Figure 5.27, it is seen again that two objects can only be distinguished when they are get closer to the opposite corners.

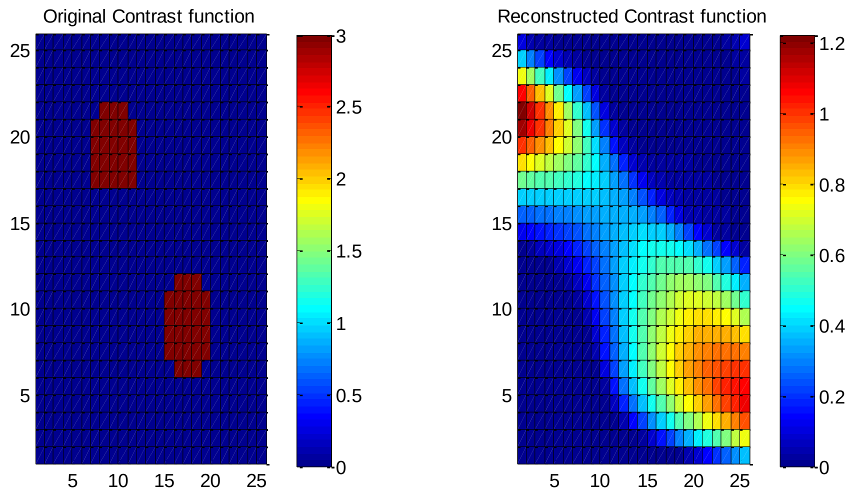

Figure 5.27 : Two objects in stratified media

6. CONCLUSIONS

The forward problems for objects located in infinite medium and three part planarly layered media is solved using MOM. The results obtained from the MOM solution are compared against to available analytical solutions and the FEM solution. Obtained results showed that there is nothing looking wrong in the forward solution.

The Contrast Source Inversion method is applied to reconstruct objects located in infinite medium, first. Then, the method is applied to reconstruct objects located in three part planarly layered media. The method is tested for different cases. It is seen that reconstruction performance is degraded for the objects located in stratified media comparing to objects in infinite medium. However, it is seen that the objects located in three part layered media can be reconstructed well using the contrast source inversion method.

How close objects can be distinguished is investigated. It is seen that when the domain size is reduced, the resolution is increased and the objects' image become separated more. As a numerical example, 0.2λ separated objects could not be distinguished when the reconstruction domain size is chosen 0.4λ. When the domain size is reduced to 0.3λ, the resolution is increased and the objects' separation becomes more clear. Furthermore, it is seen that two objects can only be distinguished when they are get close to the opposite corners of the reconstruction domain, otherwise one object overshadows the other object and their image become merged.

How small objects can be detected is investigated. It is observed that while objects get smaller, reconstruction of electrical properties become inaccurate but objects' location can be detected. As a numerical example, in 0.4λx0.4λ reconstruction domain, objects having radius of 0.12λ or greater can be reconstructed well with their electrical properties. On the other hand, objects having radius of less than 0.1λ can only be detected.

It is deduced that for the objects having either much greater permittivity than background media or so close to the background media the reconstruction performance worsens and object’s image slightly shifts up or down. The best results are obtained for the contrasts being around three. It is also seen that different arrangements for the receive points i.e. linear or half circular do not alter the reconstruction performance much.

It had been intended to solve the forward problem for three part media using FEM which is an entirely different method from MOM in order to make a legitimate study on the inverse problem. However, FEM solutions could not be obtained for three part media and MOM is used in both the forward and the inverse problems. This risks the robustness of the work. Nevertheless, contrast source inversion method is applied and examined for three part planarly layered media.

REFERENCES

[1] Roger A.(1981), Newton-Kantorovich Algorithm Applied to an Electromagnetic Inverse Problem, , IEEE Trans. on Antennas and Prop, Vol.29 (2), p.232-238.

[2] Kleinman R. E and Van den Berg P. M (1992), A Modified Gradient Method for 2-Dimensioanl Problems in Tomography, Journal of Computational and Applied Mathematics, Vol.41 (1), p.17-35.

[3] Van den Berg P. M. and Kleinman R. E. (1997), A contrast source inversion method, Inverse Problems, vol. 13, pp. 1607–1620.

[4] Van den Berg P. M., Non-linear scalar inverse scattering: algorithms and applications, Scattering, R. Pike and P. C. Sabatier (eds.), Chapter 1.3.3., Academic Press, London.

[5] Hecht Frederic (2010), FreeFEM++, Numerical Mathematics and Scientific Computation. Laboratoire J.L. Lions, http://www.freefem.org/, 3.7 edition

[6] Peterson A. F., Ray S.L., Mittra R.(1998). Computational Methods for Electromagnetics, WILEY-IEEE Press.

[7] Richmond J.A.(1965). Scattering by a dielectric cylinder of arbitrary cross section shape, IEEE Trans. on Antennas and Prop, Vol.13 (3), p.334-341.

[8] N. Kinayman and M. I. Aksun (2005), Modern Microwave Circuits. Chapter 3, Artech House, Boston.

[9] Felsen, LB. and Marcuvitz, N. (1973). Radiation and Scattering of Waves, Prentice Hall, New Jersey.

[10] Yarar L.(2009). Tabakalı Ortamlara Gömülü Cisimlere İlişkin Ters Saçılma Problemleri(Msc Thesis), İstanbul Technical University Graduate School of Science Engineering and Technology, İstanbul.

[11] Paris D. T. and Hurd F. K.(1969), Basic Electromagnetic Theory, McGraw-Hill, New York.

CURRICULUM VITAE

Name Surname: Fatih Erdem

Place and Date of Birth: Ordu, 1987

Address: TUBITAK-UEKAE, KOCAELI

E-Mail: ferdem@itu.edu.tr

B.Sc.: Yeditepe University, Dept. of Electrical-Electronics Engineering

Professional Experience:

February 2011 - : Researcher, TUBITAK-UEKAE, KOCAELI

February 2010 - February 2011 : Research Assistant, Dept. of Electronics and Telecommunication Engineering, ITU, ISTANBUL

Rewards:

2009- 2011: TUBITAK-BIDEB, Scholar

2004- 2009: Yeditepe University, Dept. of Electrical-Electronics Engineering Scholar

2004- 2009: Yeditepe University, Dept. of Electrical-Electronics Engineering Dean's List, 2 times